Research Square

Preprints are preliminary reports that have not undergone peer review.
They should not be considered conclusive, used to inform clinical practice,
or referenced by the media as validated information.

Epicardial adipose tissue volume and the Naples Prognostic Score add incremental value to EuroSCORE II for predicting MACE after TAVR: a retrospective cohort study

Bo Chen
Affiliated Hospital of Qingdao University
Xinran Li
Affiliated Hospital of Qingdao University
Kaiyuan Li
Affiliated Hospital of Qingdao University
Chi Zhou
Affiliated Hospital of Qingdao University
Zongyi Xia
Affiliated Hospital of Qingdao University
Zhexun Lian
lianzx566@163.com

Affiliated Hospital of Qingdao University

Research Article

Keywords: Calcific aortic stenosis, Epicardial adipose tissue, Major adverse cardiovascular events, Naples prognostic score, Transcatheter aortic valve replacement

Posted Date: November 9th, 2026

DOI: https://doi.org/10.21203/rs.3.rs-11411511/v1

License: This work is licensed under a Creative Commons Attribution 4.0 International License.
Read Full License

Additional Declarations: No competing interests reported.

Title

Epicardial adipose tissue volume and the Naples Prognostic Score add incremental value to EuroSCORE II for predicting MACE after TAVR: a retrospective cohort study

Authors

Bo Chen, MD[1], Xinran Li, MD[2], Kaiyuan Li, PhD[1], Chi Zhou, PhD[1], Zongyi Xia, PhD[1] and Zhexun Lian, PhD[1]*

Affiliations

[1] Department of Cardiology, the Affiliated Hospital of Qingdao University, Qingdao, Shandong 266003, China

[2] Department of Emergency Internal Medicine, the Affiliated Hospital of Qingdao University, Qingdao, Shandong 266003, China

Corresponding author

Zhexun Lian, PhD, Department of Cardiology, the Affiliated Hospital of Qingdao University, Qingdao, Shandong 266003, China. E-mail: lianzx566@163.com; Tel: +86 18661807670; ORCID: 0000-0002-0887-017X

Abstract

Background Calcific aortic valve disease (CAVD) is a common degenerative valvular disease in the elderly, and transcatheter aortic valve replacement (TAVR) is now its mainstream treatment. Conventional risk scores based on demographic and comorbidity data do not capture local cardiac inflammation or systemic nutritional status, limiting prediction of major adverse cardiovascular events (MACE) after TAVR. Epicardial adipose tissue (EAT) volume and the Naples Prognostic Score (NPS) reflect these dimensions, but their combined

incremental value is unknown. We assessed their independent and incremental value for MACE after TAVR, using EuroSCORE II as reference.

Methods In this single-center retrospective cohort study, 427 consecutive patients with severe CAVD undergoing TAVR (January 2020 to July 2025) were enrolled. EAT volume was quantified on computed tomography angiography and dichotomized at the cohort median; NPS was derived from routine laboratory indices and categorized as low (0–2) or high (3–4). The endpoint was MACE after TAVR, defined by Valve Academic Research Consortium 3 criteria. Multivariable Cox regression assessed independent prognostic value; nested models were compared by Harrell's C-index, time-dependent ROC, net reclassification index (NRI), integrated discrimination improvement (IDI) and decision curve analysis. Proportional hazards were assessed.

Results During a median follow-up of 24.51 months, 89 patients (20.8%) experienced MACE. After adjustment, both high EAT and high NPS were independent predictors, with average hazard ratios (HRs) of 3.01 (95% confidence interval (CI) 1.80–5.03; $P < 0.001$) and 1.96 (95% CI 1.27–3.04; $P = 0.003$). Adding both markers raised the C-index from 0.716 to 0.751 (likelihood-ratio $P < 0.001$); the 24-month area under the curve was 0.757. Integrated discrimination improvement was 0.068 (95% CI 0.031–0.134; $P = 0.011$) and net reclassification index was 0.075 (95% CI −0.081–0.239; $P = 0.345$). Calibration and sensitivity analyses supported the model; time-varying analysis showed that the effect of high EAT increased over follow-up whereas that of high NPS was confined to the early period.

Conclusions Preoperative EAT volume and NPS are independent, complementary predictors of MACE after TAVR. Their combination improves on conventional risk scores and requires only routine preoperative examinations.

Keywords: Calcific aortic stenosis; Epicardial adipose tissue; Major adverse cardiovascular events; Naples prognostic score; Transcatheter aortic valve replacement

Background

Calcific aortic valve disease (CAVD) is the most common valvular heart disease in the elderly population. Its pathological essence is left ventricular outflow tract obstruction caused by progressive fibrosis and calcific thickening of valve leaflets, which results from the combined effects of aging, metabolic disorders and chronic inflammation [1–3]. The Global Burden of Disease study showed that calcific aortic valve disease caused approximately 102,700 deaths and affected 12.6 million people worldwide in 2017. In developed countries, the prevalence reaches 1.7% in people aged over 65 years and exceeds 12% in those aged over 75 years, and the prevalence continues to rise with the acceleration of population aging [4]. Aortic stenosis progresses insidiously, and once symptoms appear, the natural prognosis deteriorates dramatically. The 1-year mortality rate can reach 50% in patients with severe symptomatic aortic stenosis who do not receive valve replacement intervention, with a median survival of only 2 to 5 years and a significantly increased risk of sudden death [5, 6]. Surgical aortic valve replacement has long been the standard treatment for severe aortic stenosis, but elderly patients with multiple comorbidities and high surgical risk are often intolerant to surgery, leaving a huge unmet clinical need.

The emergence of transcatheter aortic valve replacement (TAVR) has transformed the treatment of aortic stenosis, with indications broadening from surgically high-risk or inoperable patients to intermediate- and low-risk populations. The 2021 guidelines of the European Society of Cardiology (ESC) and the European Association for Cardio-Thoracic Surgery (EACTS) recommended TAVR as first-line therapy for patients aged ≥ 75 years or at high surgical risk [7], and the 2025 update lowered the preferred age threshold to ≥ 70 years for anatomically suitable patients [8]. Randomized evidence supports this expansion: the 10-year NOTION results showed long-term outcomes comparable to surgery in low- and intermediate-risk patients [9], and the EARLY TAVR trial showed that early intervention in

asymptomatic severe aortic stenosis reduced the composite endpoint of death, stroke and cardiovascular rehospitalization [10]. As indications have widened, the treated population has become increasingly heterogeneous, making accurate preoperative risk stratification and individualized decision-making increasingly important.

Currently, commonly used surgical risk scores such as EuroSCORE II and Society of Thoracic Surgeons Predicted Risk of Mortality (STS-PROM) are mainly constructed based on demographic characteristics and comorbidities. Originally developed for perioperative risk assessment of cardiac surgery, they have limited predictive performance when applied to TAVR populations. A large-scale external validation study including 2,946 German patients showed that the discriminative power of 6 commonly used risk scores for 30-day mortality after TAVR did not exceed 0.67, and there was a general phenomenon of overestimating risk with poor calibration [11]. Long-term follow-up of high-risk patients from the UK TAVR Registry also showed that long-term survival after TAVR is mainly determined by baseline comorbidities, cardiac function and other intrinsic factors, with limited independent influence of procedure-related variables, and traditional scores have limited predictive value for long-term outcomes [12]. Recently developed TAVR-specific scores such as the PRE-TAVR model, which incorporate variables such as New York Heart Association (NYHA) class, chronic obstructive pulmonary disease (COPD), C-reactive protein and transvalvular pressure gradient, can achieve an AUC of 0.77 for 1-year mortality, which is superior to traditional scores. However, the included variables are complex, and some indicators are not routine preoperative tests, resulting in limited clinical popularity [13]. Overall, existing risk scores insufficiently capture heterogeneous factors such as local cardiac remodeling, systemic inflammatory status and nutritional reserve, which is the core reason for their limited efficacy [11, 13]. Therefore, exploring simple and accessible new biomarkers to supplement the

deficiencies of traditional risk scores has become a research hotspot in preoperative risk stratification of TAVR.

Epicardial adipose tissue (EAT) is a visceral fat depot located between the visceral pericardium and the myocardium. It shares microcirculation with the myocardium and coronary vessels without fascial barrier, and can directly act on cardiac tissue through paracrine and vasocrine pathways, serving as a key hub linking obesity, inflammation and cardiovascular diseases [14, 15]. Under physiological conditions, EAT has mechanical buffering, energy supply and brown fat-like thermogenic protective effects. Under pathological conditions, EAT volume increases, adipocyte phenotype shifts to a pro-inflammatory type, with massive macrophage infiltration, releasing various pro-inflammatory cytokines such as IL-1β, IL-6, TNF-α and MCP-1, which directly participate in pathological processes such as myocardial fibrosis, valve calcification and electrical conduction abnormalities [16–18]. Numerous studies have confirmed that EAT is closely associated with various cardiovascular diseases such as coronary atherosclerosis, atrial fibrillation and heart failure [19–21]. In patients with aortic stenosis, EAT thickness is independently correlated with the degree of valve sclerosis. Pro-inflammatory mediators secreted by EAT can directly promote osteogenic differentiation and calcification of valve interstitial cells, which is an important local driving factor for the occurrence and development of CAVD [22–24]. Consistent with this, EAT has been associated with myocardial fibrosis and left ventricular dysfunction in patients with aortic stenosis [25, 26].

In TAVR populations, the prognostic value of EAT has been gradually verified. Eberhard et al. enrolled 503 TAVR patients and first confirmed that patients with EAT volume > 130 cm^3 had a 69% higher risk of 3-year all-cause mortality [27]. A 5-year long-term follow-up study of 416 patients by Schulz et al. showed that patients with high EAT volume had significantly worse long-term prognosis, and EAT volume was an independent predictor of all-cause

mortality [28]. Salam et al. further found that after adding EAT density (reflecting the degree of fat inflammation) to the clinical baseline model, the C-index for 2-year mortality prediction increased from 0.589 to 0.628 [29]. Piña et al. confirmed that both EAT volume and density were independently associated with 4-year all-cause mortality after TAVR, independent of cardiac injury stage [30]. In addition, computed tomography (CT)-derived EAT thickness and the combined assessment of epicardial and visceral adiposity have been associated with adverse outcomes after TAVR [31–33].

The Naples Prognostic Score (NPS) was first proposed by Galizia et al. in 2017 in patients undergoing colorectal cancer surgery. It integrates four routine laboratory indicators: serum albumin, total cholesterol, neutrophil-to-lymphocyte ratio and lymphocyte-to-monocyte ratio, which simultaneously reflect the level of systemic inflammation and nutritional status. Higher scores indicate more severe inflammation and poorer nutritional reserve [34]. Due to the easy accessibility of indicators and simple calculation, it has gradually expanded to multiple disease fields in recent years. In oncology, NPS has been confirmed as an independent predictor of long-term survival in various malignant tumors such as gastric cancer, esophageal cancer, gallbladder cancer and renal cancer, with better predictive performance than traditional nutritional scores [35–38]. In the cardiovascular field, Kılıç et al. found that NPS was an independent predictor of in-hospital mortality in 496 hospitalized patients with heart failure [39]. Erdoğan et al. confirmed that patients with high NPS had significantly higher in-hospital events and long-term mortality among 1,887 patients with ST-segment elevation myocardial infarction [40].

In the TAVR field, the prognostic value of NPS has also been preliminarily verified. Çetin et al. first confirmed in a 370-patient three-center cohort that patients with high NPS had significantly higher 1-year mortality, suggesting that NPS can be used for preoperative risk stratification of TAVR [41]. Gitmez et al. further found that high NPS independently

predicted 1-year major adverse cardiovascular events [42]. A long-term follow-up study of 430 patients by Demirci et al. showed that the all-cause mortality rate in the high NPS group reached 87.9%, making it one of the strongest predictors of long-term mortality [43]. In addition, as a core component of NPS, the prognostic value of neutrophil-to-lymphocyte ratio (NLR) for mortality after TAVR has also been verified by meta-analysis: a systematic review including 8 studies with 9,948 patients showed that elevated preoperative NLR was significantly associated with a 37% increase in mortality [44].

Current studies have separately verified the prognostic value of EAT volume (a local imaging inflammatory marker) and NPS (a systemic inflammatory-nutritional score) for postoperative prognosis after TAVR, but the incremental predictive value of their combination has not been reported. From the pathophysiological perspective, the two have clear complementarity: EAT volume reflects local cardiac fat load and paracrine inflammatory level, directly assessing the degree of target organ damage; NPS reflects systemic immune inflammatory activation and nutritional reserve, assessing overall tolerance of the body. The two assess patient risk from the dimensions of local organ and systemic system respectively [14, 45]. González et al. also observed a correlation between EAT volume and serum albumin level, suggesting an interaction between local fat inflammation and systemic nutritional-inflammatory axis, further supporting the theoretical basis for combined exploration [46].

Based on this background and pathophysiological rationale, this study hypothesized that both preoperative EAT volume and NPS are independent predictors of MACE after TAVR in patients with severe aortic stenosis. They provide complementary prognostic information from the dimensions of local cardiac inflammation and systemic nutritional inflammation respectively, and their combined application can produce significant incremental predictive value on the basis of traditional clinical risk scores. The purposes of this study were: (1) To verify the independent predictive value of preoperative EAT volume and NPS for MACE

after TAVR in patients with severe aortic stenosis; (2) To evaluate the incremental predictive performance of their combination on the traditional clinical risk score EuroSCORE II; (3) To provide a new combined tool for simple preoperative risk stratification of TAVR.

Methods

Study design and ethics

This single-center retrospective cohort study was conducted at the Affiliated Hospital of Qingdao University and approved by the Medical Ethics Committee of the hospital (approval No. QYFYWZLL50843). The study strictly followed the ethical principles of the Declaration of Helsinki and the Strengthening the Reporting of Observational Studies in Epidemiology (STROBE) reporting guidelines [47]. Since the study was a retrospective analysis, all data were derived from routine clinical practice and anonymized, involving no additional risk to patients or privacy disclosure. Therefore, informed consent was waived.

Study population

A total of 472 consecutive patients with severe aortic stenosis who underwent TAVR at our hospital from January 2020 to July 2025 were initially screened. Patients were excluded step by step according to the exclusion criteria: 8 patients with valvular disease who had previously received TAVR; 7 patients with acute myocardial infarction, active infection or active malignant tumor within 3 months before surgery; 28 patients with poor CT image quality that precluded EAT measurement or missing key data; 2 patients lost to follow-up after surgery. Finally, 427 patients meeting the inclusion and exclusion criteria were enrolled (Fig. 1).

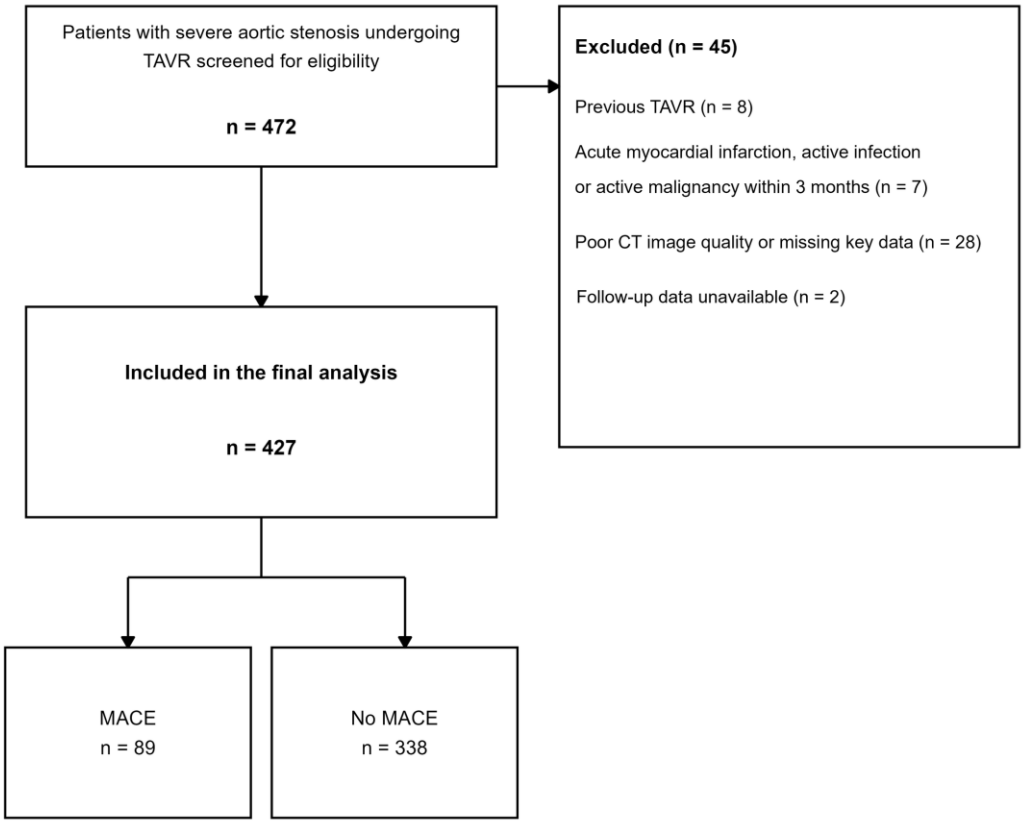


Fig. 1 Flow diagram of patient screening and inclusion. TAVR, transcatheter aortic valve replacement.

Inclusion criteria

Patients with aortic stenosis presenting with clinical symptoms such as chest pain, dyspnea and syncope; meeting the echocardiographic diagnostic criteria for severe aortic stenosis: aortic valve peak velocity > 4.0 m/s, or mean transvalvular pressure gradient ≥ 40 mmHg (1 mmHg = 0.133 kPa), or valve area < 1.0 cm^2; or effective aortic valve area index < 0.6 cm^2/m^2; assessed by the multidisciplinary heart team as suitable for TAVR on the basis of anatomical suitability, frailty, comorbidity and patient preference, and who underwent TAVR. All patients underwent TAVR successfully via the femoral approach. Complete computed tomography angiography (CTA) images within 3 months before surgery were available for epicardial adipose tissue volume measurement. Complete results of routine blood tests and

biochemistry tests within 1 week before surgery were available for calculating the Naples Prognostic Score (NPS).

Exclusion criteria

Patients were excluded if they had a malignant tumor, active infection or active autoimmune disease; had previously undergone TAVR; had congenital aortic stenosis; had combined severe mitral stenosis; or had hypertrophic cardiomyopathy with left ventricular outflow tract obstruction, pericardial disease (constrictive pericarditis or massive pericardial effusion) affecting EAT volume measurement, missing coronary CTA data, or had been lost to follow-up.

Data collection

Baseline clinical, imaging, laboratory and surgical data were retrospectively collected through the hospital electronic medical record system, imaging system and laboratory system.

Baseline clinical data

Data collected included demographic characteristics (sex, age, body mass index (BMI), smoking history, NYHA class), past medical history (hypertension, diabetes, hyperlipidemia, chronic pulmonary disease, cerebrovascular disease, atrial fibrillation history, myocardial infarction history, previous percutaneous coronary intervention (PCI) history), echocardiographic indicators (bicuspid aortic valve, left ventricular ejection fraction (LVEF), Doppler velocity index (DVI), peak aortic valve velocity, peak transvalvular pressure gradient, mean transvalvular pressure gradient, aortic valve area, pulmonary artery systolic pressure), surgical data (type of implanted valve), and laboratory indicators (white blood cells, neutrophils, lymphocytes, monocytes, hemoglobin, platelets, NLR, lymphocyte-to-monocyte ratio (LMR), D-dimer, NT-proBNP, albumin, HDL-C, LDL-C, lipoprotein(a), Cr, estimated glomerular filtration rate (eGFR)). The Doppler velocity index (DVI) is the ratio of the left ventricular outflow tract velocity-time integral to the aortic valve velocity-time integral

(equivalently, the ratio of the corresponding peak velocities), a dimensionless measure of the hemodynamic severity of aortic stenosis; a DVI below 0.25 is consistent with severe stenosis.

CT image acquisition

CTA images of all enrolled patients were acquired preoperatively. CT examination was performed with a 128-slice dual-source multislice spiral CT scanner (Revolution CT; GE MEDICAL SYSTEMS) with contrast-enhanced scan. The contrast medium dosage was 100.0 mL, and the flow rate was not recorded. Scanning parameters included: tube voltage 100 kV, tube current 649 mA, rotation time 0.28 s/rotation, slice thickness 0.625 mm, interval 0.625 mm.

Epicardial adipose tissue volume measurement

EAT volume was quantified on preoperative routine aortic CTA images using a semi-automatic volumetric method (TIMESlice), the accuracy of which has been validated against manual measurement by radiology experts [48]. The software automatically defined the cardiac range (1 cm above the aortic annulus to the cardiac base), covering the total epicardial adipose tissue in line with the accepted anatomical definition for EAT quantification [49], and applied a preset adipose tissue threshold (−190 to −30 HU) together with an anatomical recognition algorithm to identify the inner edge of the visceral pericardium and the outer myocardial surface (Fig. 2A–C). Two physicians with more than 5 years of experience in cardiovascular imaging independently reviewed and corrected the boundaries, after which the software calculated the total EAT volume (Fig. 2D), converted from mm^3 to cm^3. Patients were divided into a low EAT group (≤ median) and a high EAT group (> median) according to the cohort median, consistent with previous TAVR cohort studies in which CT-derived EAT volume has typically been categorized by the median, tertiles or quartiles rather than by reference values [28, 50, 51]; a sensitivity analysis modeling EAT volume as a continuous variable yielded consistent results (Supplemental Table S1). Inter-observer agreement was assessed by the intraclass correlation coefficient (ICC), which was 0.92 (95% CI 0.88–0.95), and the average of the two measurements was used for analysis.

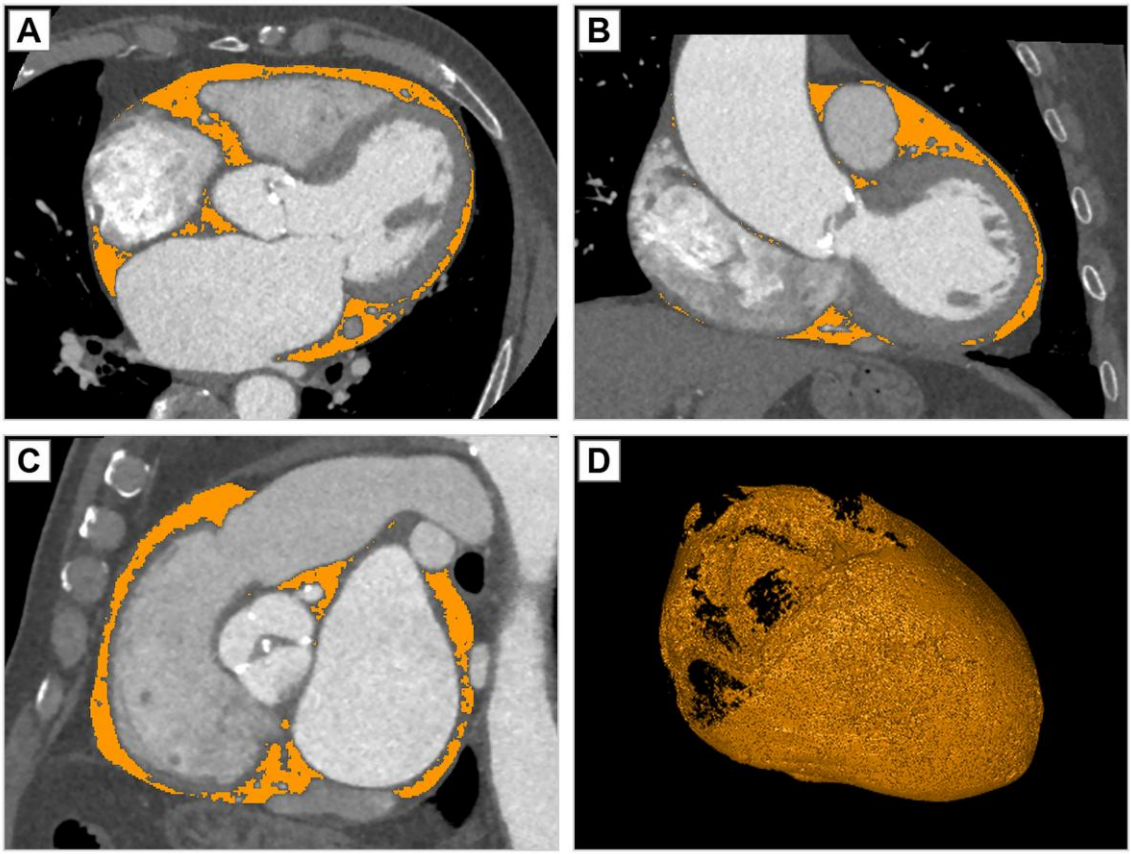


Fig. 2 Measurement of epicardial adipose tissue (EAT) volume on preoperative computed tomography angiography. (A) Axial, (B) short-axis and (C) sagittal views showing semi-automatic segmentation of EAT (orange). EAT was defined as adipose tissue between the visceral pericardium and the outer myocardial surface with an attenuation of −190 to −30 HU, and the cardiac range extended from 1 cm above the aortic annulus to the cardiac base. (D) Three-dimensional reconstruction of the segmented EAT volume, from which the total volume was calculated. CT, computed tomography; EAT, epicardial adipose tissue; HU, Hounsfield units.

Naples prognostic score calculation

Based on fasting venous blood test results within 1 week before surgery, the total NPS was calculated using the established criteria, comprising four indicators, with 1 point for each abnormality, total score 0–4: serum albumin < 4 g/dL; total cholesterol < 180 mg/dL; neutrophil-to-lymphocyte ratio (NLR) > 2.96; lymphocyte-to-monocyte ratio (LMR) ≤ 4.44. A score of 0–2 was defined as the low-NPS group, and 3–4 as the high-NPS group. The cutoff values of the four indicators used in this study are consistent with the original scoring criteria

proposed by Galizia et al. [34], and related studies in the TAVR field have all adopted the same thresholds [41–43], ensuring cross-study comparability. The optimal cutoff value fitted from the study population data was not used to avoid overfitting risk and facilitate clinical promotion.

EuroSCORE II

EuroSCORE II was calculated using the official online calculator and entered the models as a continuous variable [52].

Follow-up and endpoint

Patients were followed up through outpatient reexamination and telephone follow-up. The follow-up start point was the day of surgery, and the follow-up cutoff date was July 2026. The primary endpoint was major adverse cardiovascular events (MACE), defined according to the Valve Academic Research Consortium-3 (VARC-3) criteria [53], as a composite endpoint including all-cause death, myocardial infarction, ischemic stroke and heart failure rehospitalization. Myocardial infarction was defined as elevated myocardial injury biomarkers accompanied by symptoms of myocardial ischemia, new ischemic changes on electrocardiogram or new evidence of myocardial necrosis on imaging. Ischemic stroke was defined as new focal neurological deficit confirmed to be of ischemic etiology by imaging. Heart failure rehospitalization was defined as hospitalization due to worsening heart failure symptoms, which met the diagnostic criteria for heart failure and responded to intensified diuretic, vasodilator and other anti-heart failure treatments. The first occurrence of any of these events during follow-up was classified as MACE.

Statistical analysis

Statistical analyses were performed with R 4.5.3 (R Foundation for Statistical Computing, Vienna, Austria). All tests were two-tailed and $P < 0.05$ was considered statistically significant. Continuous variables were summarized as mean ± SD or median (interquartile

range) according to the Shapiro–Wilk test and compared with the independent-samples t test or the Mann–Whitney U test; categorical variables were summarized as n (%) and compared with the χ^2 test or Fisher exact test. Baseline characteristics were compared between patients with and without MACE. No missing values were present for any analyzed variable.

Before modeling, the correlation between the two core exposures (EAT volume and NPS) was assessed by Spearman rank correlation, and multicollinearity was assessed by the variance inflation factor (VIF), with VIF < 5 considered acceptable. Univariable Cox proportional hazards regression was first used to screen candidate variables, but covariates for the multivariable models were selected according to clinical prior knowledge rather than univariable *P* values, in order to avoid data-driven selection and over-adjustment. EuroSCORE II was used as the baseline adjustment term; hypertension, NYHA class ≥ III and the Doppler velocity index (DVI) were additionally included to account for inflammatory comorbidity, baseline cardiac function and the hemodynamic severity of aortic stenosis, respectively. Age, sex and eGFR are components of EuroSCORE II, and hemodynamic variables (valve area and peak velocity) were excluded because they are highly correlated with DVI. Four progressively nested models were constructed: Model 1 (baseline clinical model: hypertension, NYHA class ≥ III, DVI and EuroSCORE II); Models 2 and 3 (Model 1 plus high EAT and high NPS, respectively); and Model 4 (Model 1 plus both markers).

The proportional hazards (PH) assumption was tested using Schoenfeld residuals and was considered violated at $P < 0.05$. For models in which it was violated, a time-varying coefficient model was additionally fitted with $\beta(t) = \beta_0 + \beta_1 \times \log(t)$; time-specific hazard ratios were derived at 3, 6, 12, 18, 24, 36, 48 and 60 months, and this model was compared with the standard PH model by likelihood-ratio test. Hazard ratios from the standard Cox models were therefore interpreted as average effects over the follow-up period.

Model performance and incremental value were evaluated as follows: likelihood-ratio tests for nested model comparisons; Harrell's C-index for overall discrimination, with 95% CI derived from the robust standard error; time-dependent ROC curves with Kaplan–Meier marginal weighting for the 12- and 24-month AUCs; calibration curves comparing observed (Kaplan–Meier) with predicted 24-month MACE incidence across quintiles of the predicted risk, with the 95% CI of the observed estimate, assessed by the Grønnesby–Borgan (Nam–D'Agostino) goodness-of-fit test, and the calibration slope obtained by refitting a Cox model on the linear predictor; decision curve analysis across threshold probabilities; and the net reclassification index (NRI) and integrated discrimination improvement (IDI) at 24 months (tertile-based primary analysis and binary sensitivity analysis), with 95% CIs and *P* values obtained from 1,000 bootstrap resamples. Kaplan–Meier curves with the log-rank test were used to compare MACE-free survival across risk strata. The interaction between high EAT and high NPS was assessed with a product term and likelihood-ratio test, with stratified analyses. Subgroup analyses were performed for sex, age (< 75 / ≥ 75 years), NYHA class, diabetes and aortic valve anatomy, using the likelihood-ratio test for interaction. Restricted cubic splines (3 knots at the 10th, 50th and 90th percentiles of EAT volume, with the median as reference) were used to assess the dose–response relationship between EAT volume and MACE. Internal validation used 1,000 bootstrap resamples to derive optimism-corrected C-index and 24-month AUC values. Sensitivity analyses excluded 30-day perioperative events and modeled EAT volume as a continuous variable. With 89 events and 6 variables in the final model (event-to-variable ratio ≈ 14.8:1), the analysis satisfied the conventional requirement of at least 10 events per variable.

Results

Baseline characteristics

A total of 427 patients with severe aortic stenosis who underwent TAVR were enrolled. The follow-up was cut off in July 2026, with a maximum follow-up of 77.33 months and a median follow-up of 24.51 months. During follow-up, 89 patients (20.8%) experienced MACE, comprising 13 cases of all-cause death, 21 of non-fatal myocardial infarction, 19 of ischemic stroke and 36 of heart failure rehospitalization, with heart failure rehospitalization being the most frequent component. Compared with patients without MACE, patients who developed MACE were older (76.21 ± 8.00 vs 73.00 ± 6.45 years, $P < 0.001$), were more often female (48.3% vs 36.1%, $P = 0.047$), had a higher prevalence of hypertension (67.4% vs 45.0%, $P < 0.001$) and more advanced NYHA class (≥ III, 65.2% vs 48.8%, $P = 0.009$), a higher EuroSCORE II (2.67 (2.02, 4.72) vs 1.71 (1.26, 2.73), $P < 0.001$) and worse renal function (creatinine 76.00 (64.00, 108.00) vs 70.00 (60.00, 89.95) μmol/L, $P = 0.015$; eGFR 75.04 (49.84, 87.90) vs 84.69 (65.94, 92.99) mL/min/1.73 m², $P < 0.001$). With respect to aortic valve hemodynamics, the MACE group had a higher Doppler velocity index (0.22 (0.20, 0.25) vs 0.20 (0.17, 0.23), $P < 0.001$) but lower peak velocity (4.45 ± 0.63 vs 4.62 ± 0.67 m/s, $P = 0.028$), peak gradient (80.93 ± 21.23 vs 87.19 ± 25.96 mmHg, $P = 0.020$) and mean gradient (48.62 ± 14.20 vs 52.50 ± 17.53 mmHg, $P = 0.031$). Laboratory indices also differed: patients with MACE had lower hemoglobin (121.12 ± 23.20 vs 129.65 ± 18.19 g/L, $P = 0.002$), lower serum albumin (39.23 ± 3.84 vs 40.38 ± 4.01 g/L, $P = 0.014$), a lower lymphocyte-to-monocyte ratio (3.39 (2.47, 4.31) vs 3.79 (2.94, 5.15), $P = 0.002$), a higher monocyte count (0.46 (0.37, 0.62) vs 0.43 (0.35, 0.52) $\times 10^9$/L, $P = 0.018$) and lower total and LDL cholesterol (4.06 ± 1.09 vs 4.34 ± 1.17 mmol/L, $P = 0.039$; 2.27 ± 0.86 vs 2.48 ± 0.92 mmol/L, $P = 0.048$). Regarding the two core exposures, EAT volume was substantially larger in the MACE group (117.85 (108.98, 119.91) vs 104.86 (99.74, 111.14) cm³, $P < 0.001$), and the proportions of patients with high EAT (78.7% vs 42.6%) and high NPS (56.2% vs 29.9%)

were both significantly higher (both $P < 0.001$). The remaining baseline characteristics are shown in Table 1.

Table 1 Baseline characteristics of the study population stratified by MACE

		MACE events		
Baseline characteristics	**Overall (N = 427)**	**No MACE (N = 338)**	**MACE (N = 89)**	***P* value**
Age, years	73.67 ± 6.92	73.00 ± 6.45	76.21 ± 8.00	<0.001
Sex				0.047
Female	165 (38.6%)	122 (36.1%)	43 (48.3%)	
Male	262 (61.4%)	216 (63.9%)	46 (51.7%)	
BMI, kg/m²	24.24 ± 3.65	24.19 ± 3.63	24.42 ± 3.77	0.605
Smoking history	114 (26.7%)	87 (25.7%)	27 (30.3%)	0.461
Hypertension	212 (49.6%)	152 (45.0%)	60 (67.4%)	<0.001
Diabetes mellitus	122 (28.6%)	92 (27.2%)	30 (33.7%)	0.283
Hyperlipidemia	205 (48.0%)	167 (49.4%)	38 (42.7%)	0.313
Chronic lung disease	37 (8.7%)	29 (8.6%)	8 (9.0%)	>0.999
Cerebrovascular disease	53 (12.4%)	37 (10.9%)	16 (18.0%)	0.108
Atrial fibrillation	44 (10.3%)	34 (10.1%)	10 (11.2%)	0.897
Myocardial infarction	31 (7.3%)	29 (8.6%)	2 (2.2%)	0.069
Prior PCI	52 (12.2%)	41 (12.1%)	11 (12.4%)	>0.999
Bicuspid aortic valve	50 (11.7%)	42 (12.4%)	8 (9.0%)	0.476
Pulmonary hypertension	166 (38.9%)	129 (38.2%)	37 (41.6%)	0.642
NYHA class ≥ III	223 (52.2%)	165 (48.8%)	58 (65.2%)	0.009
LVEF, %	59.00 (50.00, 60.00)	59.00 (50.00, 60.75)	59.00 (53.00, 60.00)	0.878
Aortic valve peak velocity, m/s	4.58 ± 0.67	4.62 ± 0.67	4.45 ± 0.63	0.028
Peak transvalvular gradient, mmHg	85.89 ± 25.15	87.19 ± 25.96	80.93 ± 21.23	0.020
Mean transvalvular gradient, mmHg	51.69 ± 16.95	52.50 ± 17.53	48.62 ± 14.20	0.031
Doppler velocity index (DVI)	0.20 (0.17, 0.24)	0.20 (0.17, 0.23)	0.22 (0.20, 0.25)	<0.001
Aortic valve area, cm²	0.70 ± 0.18	0.70 ± 0.19	0.73 ± 0.17	0.136
WBC, ×10⁹/L	5.97 (4.96, 7.26)	5.96 (4.96, 7.27)	6.00 (4.95, 7.05)	0.974
Neutrophil count, ×10⁹/L	3.57 (2.76, 4.48)	3.60 (2.76, 4.47)	3.50 (2.76, 4.51)	0.810
Lymphocyte count, ×10⁹/L	1.62 (1.24, 2.02)	1.62 (1.27, 2.05)	1.52 (1.13, 1.84)	0.139
Monocyte count, ×10⁹/L	0.44 (0.35, 0.53)	0.43 (0.35, 0.52)	0.46 (0.37, 0.62)	0.018
Hemoglobin, g/L	127.87 ± 19.62	129.65 ± 18.19	121.12 ± 23.20	0.002
Platelet count, ×10⁹/L	187.00 (153.00, 224.00)	187.50 (153.25, 223.75)	187.00 (148.00, 229.00)	0.977
NLR	2.15 (1.61, 2.94)	2.13 (1.58, 2.87)	2.31 (1.68, 3.31)	0.196
LMR	3.68 (2.83, 4.92)	3.79 (2.94, 5.15)	3.39 (2.47, 4.31)	0.002
D-dimer, ng/mL	370.00 (310.00, 490.00)	370.00 (310.00, 480.00)	370.00 (300.00, 520.00)	0.802
NT-proBNP, pg/mL	1,254.50 (408.90, 3,768.50)	1,249.25 (395.02, 3,722.00)	1,275.00 (563.00, 3,802.00)	0.547
Serum albumin, g/L	40.14 ± 4.00	40.38 ± 4.01	39.23 ± 3.84	0.014
Triglycerides, mmol/L	0.97 (0.73, 1.38)	0.96 (0.73, 1.38)	1.01 (0.73, 1.29)	0.941
Total cholesterol, mmol/L	4.28 ± 1.16	4.34 ± 1.17	4.06 ± 1.09	0.039
HDL-C, mmol/L	1.24 ± 0.34	1.25 ± 0.33	1.20 ± 0.34	0.225
LDL-C, mmol/L	2.44 ± 0.91	2.48 ± 0.92	2.27 ± 0.86	0.048
Lipoprotein(a), mg/L	168.00 (95.00, 405.35)	172.00 (88.93, 407.88)	163.00 (99.00, 387.00)	0.995
Cr, μmol/L	71.00 (60.00, 92.00)	70.00 (60.00, 89.95)	76.00 (64.00, 108.00)	0.015
eGFR, mL/min/1.73 m²	83.35 (64.29, 91.76)	84.69 (65.94, 92.99)	75.04 (49.84, 87.90)	<0.001
Prosthesis type				0.114
Balloon-expandable	69 (16.2%)	60 (17.8%)	9 (10.1%)	
Self-expanding	358 (83.8%)	278 (82.2%)	80 (89.9%)	
EuroSCORE II, %	1.95 (1.34, 3.26)	1.71 (1.26, 2.73)	2.67 (2.02, 4.72)	<0.001
Epicardial adipose tissue volume, cm³	107.23 (100.46, 112.73)	104.86 (99.74, 111.14)	117.85 (108.98, 119.91)	<0.001
High EAT	214 (50.1%)	144 (42.6%)	70 (78.7%)	<0.001
High NPS	151 (35.4%)	101 (29.9%)	50 (56.2%)	<0.001

Data are presented as mean ± SD, median (IQR), or n (%). Continuous variables were compared using the independent-samples t test or the Mann–Whitney U test, and categorical variables using the Pearson χ^2 test or Fisher exact test, as

appropriate. BMI, body mass index; CI, confidence interval; Cr, creatinine; CT, computed tomography; eGFR, estimated glomerular filtration rate; HDL-C, high-density lipoprotein cholesterol; IQR, interquartile range; LDL-C, low-density lipoprotein cholesterol; LMR, lymphocyte-to-monocyte ratio; LVEF, left ventricular ejection fraction; MACE, major adverse cardiovascular events; NLR, neutrophil-to-lymphocyte ratio; NPS, Naples prognostic score; NT-proBNP, N-terminal pro-B-type natriuretic peptide; NYHA, New York Heart Association; PCI, percutaneous coronary intervention; SD, standard deviation; WBC, white blood cell count.

Univariable Cox regression analysis

Univariable Cox proportional hazards regression showed that a total of 17 baseline variables were statistically associated with MACE risk after TAVR (all $P < 0.05$), including age, sex, hypertension, NYHA class ≥ III, Doppler velocity index (DVI), valve area, peak pressure gradient, peak velocity, mean pressure gradient, lymphocyte-to-monocyte ratio (LMR), serum albumin, eGFR, hemoglobin, EuroSCORE II score, EAT volume, high EAT group and high NPS group. The crude effect of core study indicators showed that the risk of MACE in the high EAT group was 3.84 times that in the low EAT group (HR 3.84, 95% CI 2.31–6.38, $P < 0.001$); the risk in the high NPS group was 2.64 times that in the low NPS group (HR 2.64, 95% CI 1.73–4.03, $P < 0.001$). Detailed results are shown in Table 2.

Table 2 Univariable Cox regression analysis for MACE after TAVR

Variable	HR (95% CI)	*P* value
Age, years	1.06 (1.03–1.10)	<0.001
Sex (male vs female)	0.60 (0.40–0.91)	0.017
Hypertension	2.47 (1.58–3.86)	<0.001
NYHA class ≥ III	1.78 (1.15–2.76)	0.009
Aortic valve peak velocity, m/s	0.69 (0.51–0.94)	0.019
Peak transvalvular gradient, mmHg	0.99 (0.98–1.00)	0.020
Mean transvalvular gradient, mmHg	0.98 (0.97–1.00)	0.026
DVI, per 0.1 unit	1.55 (1.28–1.88)	<0.001
Aortic valve area, cm²	3.23 (1.09–9.59)	0.034
Hemoglobin, g/L	0.98 (0.97–0.99)	<0.001
Serum albumin, g/L	0.94 (0.90–0.99)	0.024
eGFR, mL/min/1.73 m²	0.99 (0.98–0.99)	0.002
EuroSCORE II, per 1% increase	1.15 (1.09–1.21)	<0.001
EAT volume, cm³	1.01 (1.01–1.02)	<0.001
High EAT	3.84 (2.31–6.38)	<0.001
High NPS	2.64 (1.73–4.03)	<0.001

Only variables with P < 0.05 are shown; the complete analysis of all 44 candidate variables is presented in Supplementary Table S2. CI, confidence interval; DVI, Doppler velocity index; EAT, epicardial adipose tissue; eGFR, estimated glomerular filtration rate; HR, hazard ratio; LMR, lymphocyte-to-monocyte ratio; MACE, major adverse cardiovascular events; NPS, Naples prognostic score; NYHA, New York Heart Association; TAVR, transcatheter aortic valve replacement. Hazard ratios for the Doppler velocity index are expressed per 0.1-unit increase. Hazard ratios for sex are expressed as male versus female (female as reference).

Multivariable Cox regression

EAT volume and NPS were only weakly correlated (Spearman $r_s = 0.175$ for EAT volume vs. the high NPS category, $P < 0.001$), indicating limited information overlap and a complementary basis for their combined use. All variables in the model had VIF < 1.13, with no significant multicollinearity (Supplemental Table S3). Schoenfeld residual testing showed that Models 1 and 3 met the proportional hazards assumption (global $P = 0.131$ and 0.098), whereas Models 2 and 4 deviated (global $P = 0.006$ and 0.003), driven by the high EAT variable (residual $P = 0.010$ and 0.009; Supplemental Tables S4 and S5). The time-dependent behavior of the two markers differed: the effect of NPS was more prominent early after surgery and weakened thereafter, whereas the EAT hazard ratio increased progressively with follow-up. The hazard ratios from the standard Cox models should therefore be interpreted as average effects over the entire follow-up period, with the core efficacy evaluation based on the time-specific estimates presented in the time-varying analysis below. After adjustment for hypertension, NYHA class ≥ III, DVI and EuroSCORE II, both high EAT and high NPS remained independent predictors of MACE. In the baseline + high EAT model the adjusted HR for high EAT was 3.23 (95% CI 1.94–5.40, $P < 0.001$), and in the baseline + high NPS model the adjusted HR for high NPS was 2.21 (95% CI 1.43–3.44, $P < 0.001$). In the combined model, the adjusted HRs were 3.01 (95% CI 1.80–5.03, $P < 0.001$) for high EAT and 1.96 (95% CI 1.27–3.04, $P = 0.003$) for high NPS (Table 3).

Table 3 Sequential Cox proportional hazards models for MACE after TAVR

Model	Variable	HR (95% CI)	*P* value
Model 1: Base model	Hypertension	1.99 (1.25–3.16)	0.004
	NYHA class ≥ III	1.73 (1.11–2.72)	0.016
	DVI, per 0.1 unit	1.55 (1.25–1.91)	<0.001
	EuroSCORE II, per 1% increase	1.13 (1.07–1.19)	<0.001
Model 2: Base + high EAT	Hypertension	2.06 (1.30–3.27)	0.002
	NYHA class ≥ III	1.52 (0.96–2.39)	0.073
	DVI, per 0.1 unit	1.49 (1.22–1.82)	<0.001
	EuroSCORE II, per 1% increase	1.13 (1.06–1.21)	<0.001
	High EAT	3.23 (1.94–5.40)	<0.001
Model 3: Base + high NPS	Hypertension	2.12 (1.33–3.37)	0.002
	NYHA class ≥ III	1.71 (1.09–2.69)	0.019
	DVI, per 0.1 unit	1.45 (1.18–1.79)	<0.001
	EuroSCORE II, per 1% increase	1.10 (1.04–1.16)	0.002
	High NPS	2.21 (1.43–3.44)	<0.001

Model	Variable	HR (95% CI)	*P* value
Model 4: Combined model	Hypertension	2.11 (1.33–3.35)	0.001
	NYHA class ≥ III	1.49 (0.94–2.35)	0.088
	DVI, per 0.1 unit	1.41 (1.15–1.73)	<0.001
	EuroSCORE II, per 1% increase	1.11 (1.03–1.19)	0.006
	High EAT	3.01 (1.80–5.03)	<0.001
	High NPS	1.96 (1.27–3.04)	0.003

CI, confidence interval; DVI, Doppler velocity index; EAT, epicardial adipose tissue; HR, hazard ratio; MACE, major adverse cardiovascular events; NPS, Naples prognostic score; NYHA, New York Heart Association; TAVR, transcatheter aortic valve replacement. Hazard ratios for the Doppler velocity index are expressed per 0.1-unit increase. The proportional hazards assumption was met in Models 1 and 3 (global Schoenfeld residual test P = 0.131 and 0.098) and violated in Models 2 and 4 (P = 0.006 and 0.003); the hazard ratios for Models 2 and 4 therefore represent average effects over the follow-up period. Time-specific hazard ratios are presented in Supplementary Table S6.

Validation of combined prediction model performance

Overall discriminative ability (C-index)

For overall discriminative ability, the Harrell's C-index of the baseline clinical model was 0.716 (95% CI 0.654–0.777). After adding the high EAT group to the baseline model, the C-index increased to 0.727 ($\chi^2 = 24.21$, $P < 0.001$ for likelihood ratio test). After adding the high NPS group, the C-index was 0.738 ($\chi^2 = 12.55$, $P < 0.001$ for likelihood ratio test). The Harrell's C-index of the combined prediction model was 0.751 (95% CI 0.692–0.809), with an absolute increase of 0.035 compared with the baseline model 0.716 (95% CI 0.654–0.777). The difference was statistically significant by likelihood ratio test ($\chi^2 = 33.33$, $P < 0.001$). After bootstrap internal validation and optimism bias correction, the C-index of the combined model still reached 0.742, indicating stable discriminative ability. Detailed results are shown in Table 4, Panel A.

Table 4 Incremental predictive performance of the nested models and added value of the combined model

A. Discrimination across the nested models

Model	C-index (95% CI)	12-month AUC	24-month AUC	Likelihood-ratio χ^2 (*P* value)
Model 1: Base model	0.716 (0.654–0.777)	0.733	0.716	—
Model 2: Base + high EAT	0.727 (0.665–0.789)	0.722	0.739	24.21 (<0.001)
Model 3: Base + high NPS	0.738 (0.680–0.797)	0.763	0.728	12.55 (<0.001)
Model 4: Combined model	0.751 (0.692–0.809)	0.755	0.757	33.33 (<0.001)

B. Incremental value of the combined model versus the base model

Method	Metric	Estimate	95% CI	*P* value
Tertile-based (primary analysis)	Event NRI	0.058	−0.176 to 0.397	0.677
	Non-event NRI	0.017	−0.224 to 0.248	0.894
	Total NRI	0.075	−0.081 to 0.239	0.345
	Total IDI	0.068	0.031–0.134	0.011

Method	Metric	Estimate	95% CI	*P* value
Binary-based (sensitivity analysis)	Event NRI	0.029	−0.104 to 0.243	0.734
	Non-event NRI	0.006	−0.168 to 0.175	0.950
	Total NRI	0.035	−0.051 to 0.175	0.543
	Total IDI	0.068	0.031–0.134	0.011

Likelihood-ratio χ^2 and P values are for each model versus Model 1 (base model). In Panel B, NRI and IDI are presented for both the tertile-based primary analysis and the binary-based sensitivity analysis. IDI is derived from continuous predicted probabilities and is therefore identical for the two categorization approaches.

AUC, area under the receiver operating characteristic curve; C-index, concordance index; CI, confidence interval; IDI, integrated discrimination improvement; MACE, major adverse cardiovascular events; NRI, net reclassification improvement.

Time-dependent ROC curves

Time-dependent ROC curve analysis showed that all models had certain predictive performance for MACE events at different time points after TAVR, and the combined prediction model had the highest discriminative ability at 24 months; at 12 months, the base + high NPS model achieved the highest AUC (0.763), slightly exceeding that of the combined model (0.755). At 12 months after surgery, the AUC of the baseline clinical model was 0.733. Adding the high NPS group increased the AUC to 0.763, whereas adding the high EAT group alone did not improve discrimination (AUC 0.722). The AUC of the combined prediction model including both reached 0.755. At 24 months after surgery, the AUC of the baseline clinical model was 0.716. After adding the high EAT group and high NPS group to the base model respectively, the AUC increased to 0.739 and 0.728, and the AUC of the combined prediction model increased to 0.757. The discriminative performance of the combined prediction model at 24 months after surgery was superior to the single-marker models and the baseline clinical model. See Table 4, Panel A, and Fig. 3 for details. Receiver operating characteristic analysis based on the binary MACE outcome over the complete follow-up period showed consistent discrimination (Supplemental Figure S1).

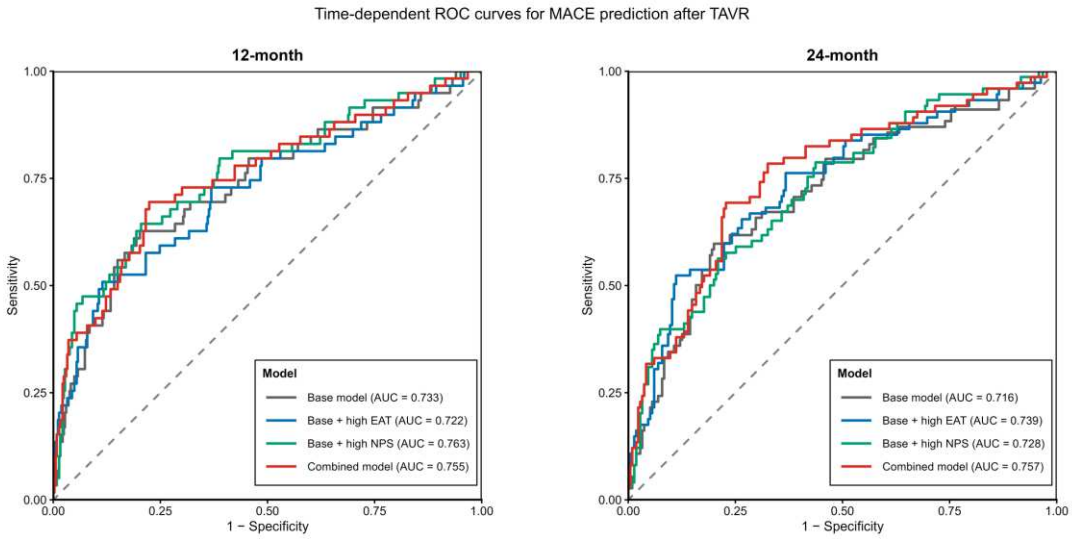


Fig. 3 Time-dependent ROC curves for MACE prediction after TAVR. The dashed diagonal line indicates chance discrimination. AUC, area under the receiver operating characteristic curve; CI, confidence interval; MACE, major adverse cardiovascular events; ROC, receiver operating characteristic; TAVR, transcatheter aortic valve replacement.

Calibration

The calibration curve was plotted using quintiles of the predicted risk to assess the consistency between the predicted probability of MACE at 24 months after TAVR by the combined prediction model and the observed event incidence. All study subjects were divided into five subgroups according to the predicted risk of the combined model, and the observed 24-month MACE incidence within each subgroup was estimated by the Kaplan–Meier method together with its 95% confidence interval. The calibration curve showed good overall agreement between the predicted probability of 24-month MACE and the observed incidence, and the 95% confidence intervals of all five subgroups included the line of perfect calibration (Fig. 4). Formal assessment confirmed adequate calibration: the Grønnesby–Borgan goodness-of-fit test gave $\chi^2 = 4.45$ (df = 4, $P = 0.349$) across quintiles ($\chi^2 = 2.05$, df = 2, $P = 0.360$ across tertiles), and the calibration slope was 1.00 (95% CI 0.78–1.22).

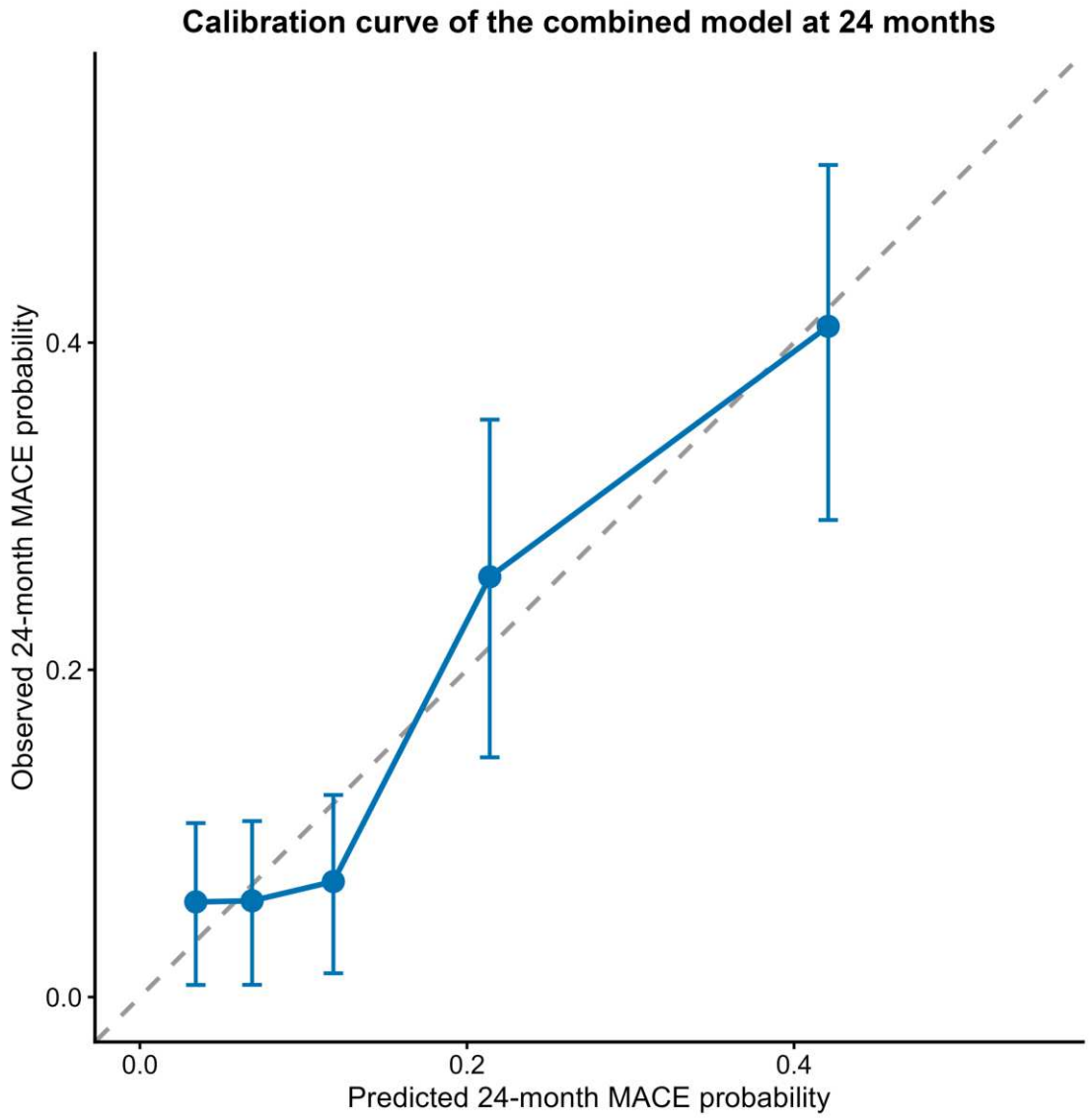


Fig. 4 Calibration curve for 24-month MACE risk of the combined model. Points represent quintiles of the predicted risk and vertical bars indicate the 95% CI of the observed (Kaplan–Meier) estimate; the dashed diagonal line indicates perfect calibration, and the 95% CI of every quintile includes this line. MACE, major adverse cardiovascular events.

Decision curve analysis

Decision curve analysis was used to evaluate the clinical net benefit of the model. Within the threshold probability range of 0 to 0.5, the prediction model combining EAT and NPS consistently achieved higher net benefit than the basic clinical model, and both models exhibited superior net benefit compared with the “treat all” and “treat none” strategies. After the threshold probability exceeded 0.10, the net benefit advantage of the combined model

remained stable. At a threshold probability of 0.50, the combined model still maintained positive net benefit, while the net benefit of the basic model approached 0, indicating that the combined model had better clinical decision-making value (Fig. 5).

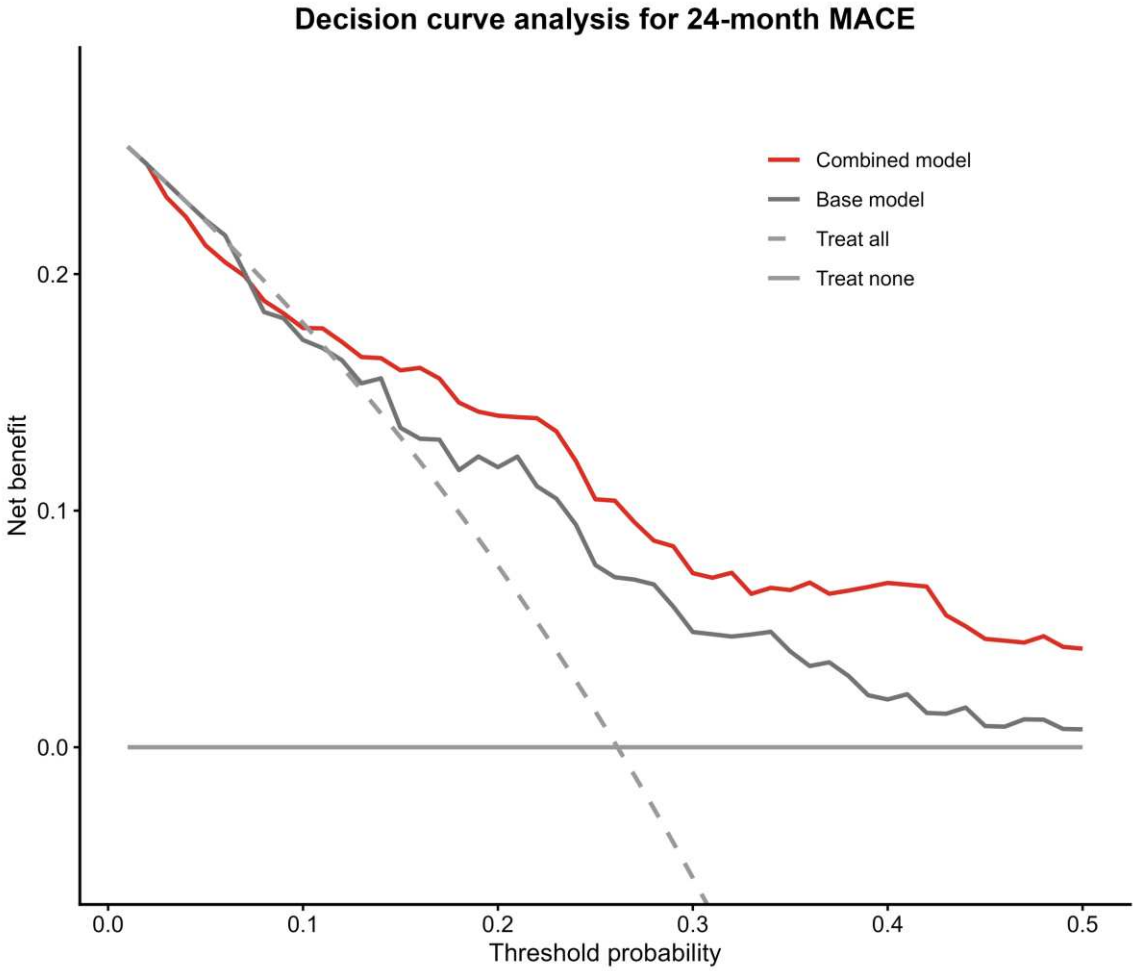


Fig. 5 Decision curve analysis for 24-month MACE prediction. Treat all and treat none represent reference strategies. DCA, decision curve analysis; MACE, major adverse cardiovascular events.

Incremental predictive value

Incremental value analysis at 24 months after surgery showed that: compared with the base clinical model, the overall integrated discrimination improvement (IDI) in the primary analysis using the tertile method for the combined prediction model was 0.068 (95% CI 0.031–0.134, $P = 0.011$), which was statistically significant, indicating that the combination of EAT and NPS could significantly improve the overall discrimination ability of the model for MACE events at 24 months after TAVR. In terms of risk reclassification, the overall net

reclassification index (NRI) using the tertile method was 0.075 (95% CI −0.081–0.239, P = 0.345), with an NRI of 0.058 in the event group and 0.017 in the non-event group. The point estimates of all indicators were positive, suggesting that the newly added indicators had a positive improving trend in the reclassification performance of patient risk stratification, but the result did not reach statistical significance. Sensitivity analysis using binary risk stratification showed that the overall NRI of the combined model was 0.035, with the same effect direction as the primary analysis, confirming that this incremental trend was relatively robust and not affected by the selection of stratification cutoff values (Table 4, Panel B).

Risk stratification survival analysis and interaction effect

On the basis of verifying the predictive performance of the model, risk stratification analysis was further used to evaluate the clinical application value of the model, and to analyze the interaction pattern of EAT and NPS on MACE prediction.

Risk stratification survival curves

According to the tertiles of the risk score of the combined prediction model, patients were divided into low-risk group (lowest tertile), intermediate-risk group (middle tertile) and high-risk group (highest tertile). Kaplan–Meier survival curves showed statistically significant differences in MACE-free survival probabilities among the three groups (log-rank $P < 0.001$), with significantly lower MACE-free survival in the high-risk group than in the intermediate and low-risk groups. See Fig. 6 for details. Separate stratification analysis showed that MACE-free survival probabilities in both high EAT group and high NPS group were significantly lower than the corresponding low groups (both $P < 0.001$), consistent with the trend of the combined model (Supplemental Figures S2 and S3).

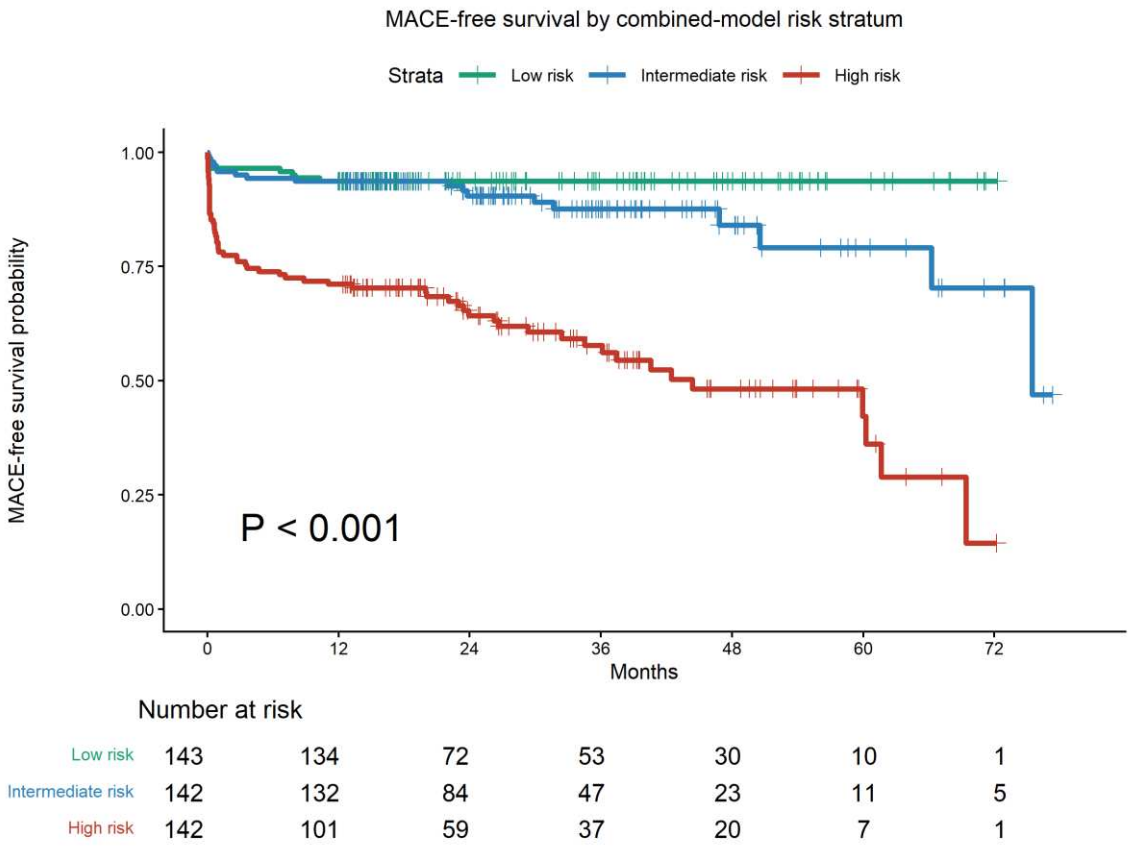


Fig. 6 Kaplan–Meier curves for MACE-free survival by combined-model risk stratum. The P value was calculated using the log-rank test. MACE, major adverse cardiovascular events.

Interaction effect of EAT and NPS

The interaction model including the product term of high EAT × high NPS gave an interaction HR of 0.54 (95% CI 0.19–1.55), with likelihood ratio test $P = 0.251$. This indicates no significant statistical interaction and an essentially additive relationship. In stratified analyses, elevated EAT was associated with higher MACE risk at both NPS levels, and elevated NPS with higher risk at both EAT levels. These estimates are imprecise in the present sample, however, and a synergistic or antagonistic effect cannot be excluded; larger cohorts will be needed to test it formally. See Table 5 for details.

Table 5 Interaction and stratified analyses of high EAT and high NPS

A. Interaction between high EAT and high NPS

Variable	HR (95% CI)	*P* value	Likelihood-ratio *P* value	Conclusion
High EAT × high NPS interaction	0.54 (0.19–1.55)	0.253	0.251	No significant interaction

B. Stratified effect estimates

Stratification	High EAT HR	95% CI	*High NPS HR*	95% CI	P value
NPS = No	3.98	1.81–8.77	—	—	<0.001
NPS = Yes	2.04	1.03–4.05	—	—	0.040
EAT = No	—	—	2.93	1.12–7.67	0.028
EAT = Yes	—	—	1.73	1.06–2.83	0.029

HRs compare the high-risk with the low-risk group within each stratum; each P value corresponds to the HR shown in the same row. CI, confidence interval; EAT, epicardial adipose tissue; HR, hazard ratio; MACE, major adverse cardiovascular events; NPS, Naples prognostic score.

Time-varying effect of EAT and NPS

Because the proportional hazards assumption was violated in the models containing EAT, the combined model was refitted with time-varying coefficients [$\beta(t) = \beta_0 + \beta_1 \times \log(t)$]. The time-varying model fitted the data significantly better than the proportional-hazards model (likelihood-ratio $\chi^2 = 9.34$, df = 2, $P = 0.009$). The effect of high EAT increased progressively over follow-up (HR 3.64 [95% CI 2.04–6.50] at 3 months; 6.20 [2.63–14.61] at 24 months; 7.84 [2.84–21.63] at 60 months; all $P < 0.001$), whereas the effect of high NPS was confined to the early postoperative period and attenuated thereafter (HR 1.89 [1.21–2.96], $P = 0.006$ at 3 months; 1.46 [0.86–2.48], $P = 0.159$ at 12 months; 1.08 [0.52–2.25], $P = 0.827$ at 60 months). These findings indicate that NPS mainly reflects early perioperative risk, whereas EAT is associated with risk accruing over long-term follow-up (Supplemental Table S6 and Fig. 7).

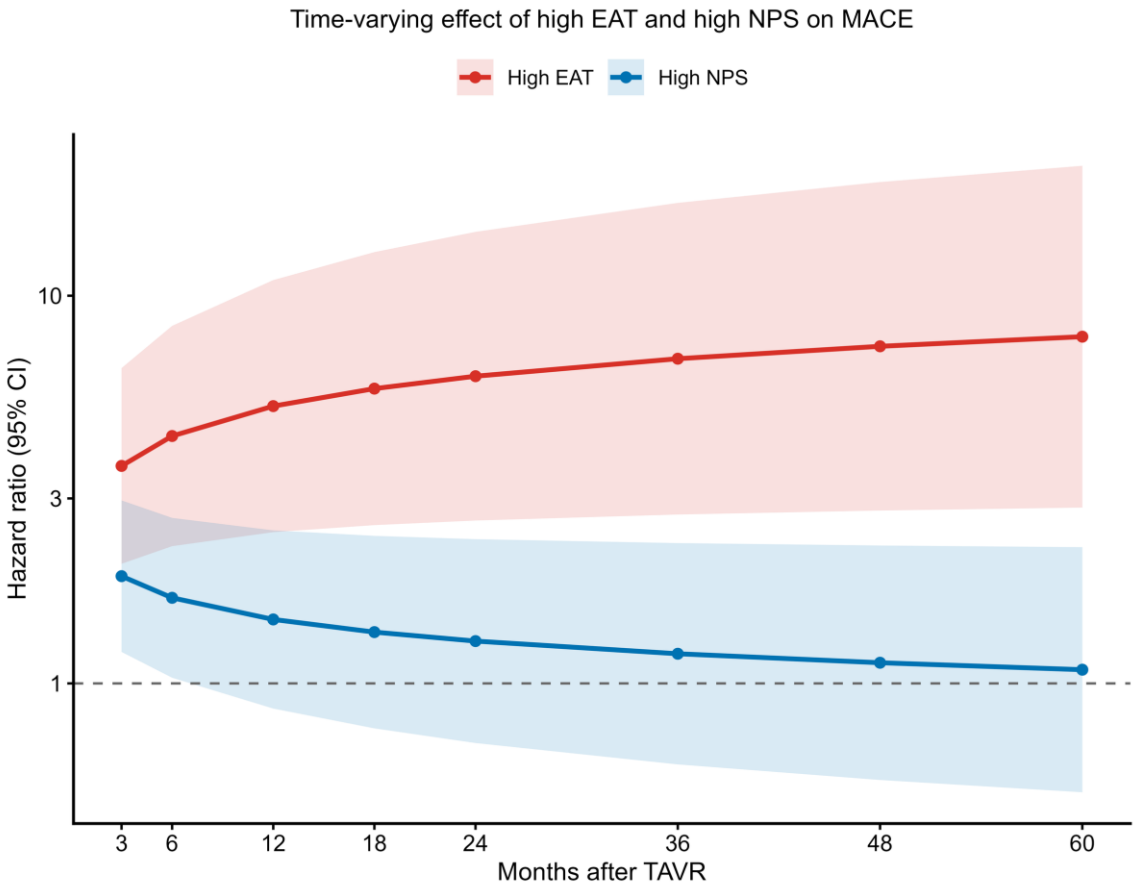


Fig. 7 Time-varying effect of high EAT and high NPS on MACE after TAVR. Hazard ratios (95% CI) were estimated at 3, 6, 12, 18, 24, 36, 48 and 60 months; the dashed line indicates a hazard ratio of 1. CI, confidence interval; EAT, epicardial adipose tissue; HR, hazard ratio; MACE, major adverse cardiovascular events; NPS, Naples prognostic score; TAVR, transcatheter aortic valve replacement.

Subgroup generalizability analysis

Subgroup stratification analysis showed that the combined model discriminated MACE risk across subgroups defined by sex, age (< 75 / ≥ 75 years), NYHA class and diabetes, with hazard ratios for the high- versus low-risk group ranging from 6.39 to 10.31 (all $P < 0.01$) and no significant interaction ($P = 0.537$, 0.672, 0.523 and 0.548, respectively). The bicuspid aortic valve subgroup had limited power (n = 50; 8 MACE events; HR 3.49, 95% CI 0.39–31.39; $P = 0.264$). See Supplemental Table S7 and Fig. 8 for details.

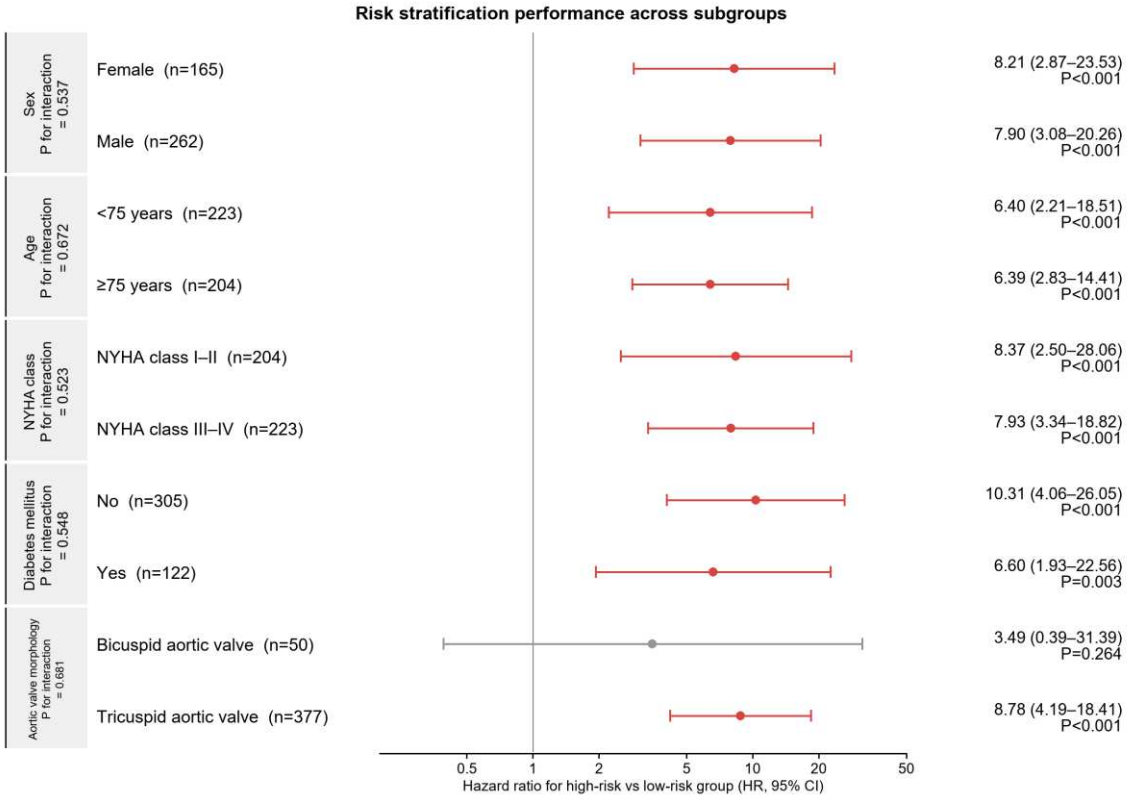


Fig. 8 Forest plot of subgroup analyses for the combined model. Hazard ratios are shown on a logarithmic scale; red indicates P < 0.05 and grey indicates P ≥ 0.05. CI, confidence interval; HR, hazard ratio.

Dose–response relationship between EAT and MACE

Restricted cubic spline analysis showed no significant nonlinearity ($P = 0.092$), indicating an approximately linear positive association between EAT volume and MACE across the observed range, with only a modest nonlinear trend (Fig. 9, Supplemental Table S8). Risk was relatively flat below the reference value and increased steadily above it, with the 95% CIs excluding 1 in the higher volume range. These results indicate a continuous dose–effect association between EAT volume and MACE after TAVR; the corresponding continuous-variable Cox model is reported in the sensitivity analysis of the exposure variable form below.

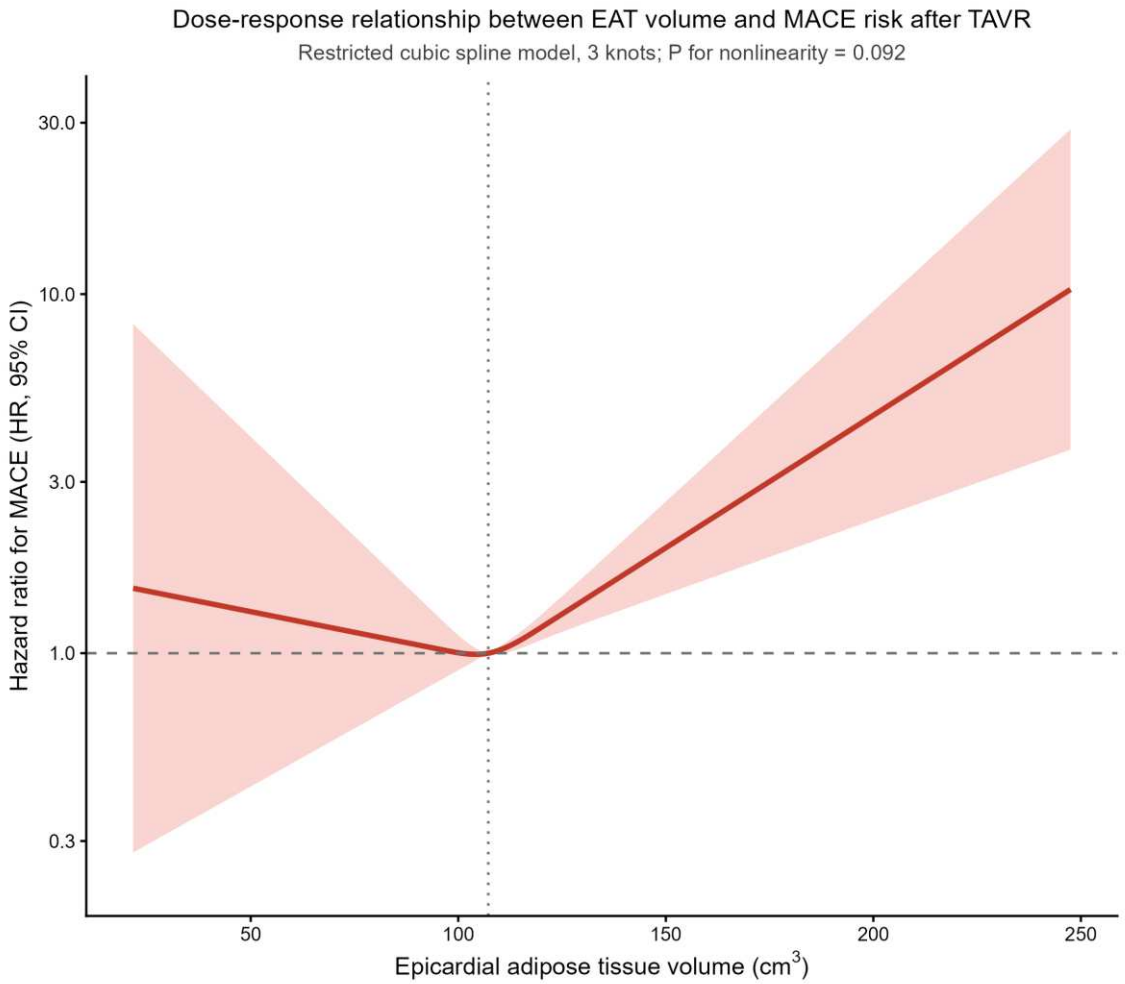


Fig. 9 Restricted cubic spline analysis of EAT volume and MACE risk after TAVR. The solid line indicates the hazard ratio; the shaded area indicates the 95% CI; the vertical dotted line marks the reference value (cohort median EAT volume, 107.23 cm³). CI, confidence interval; EAT, epicardial adipose tissue; HR, hazard ratio; MACE, major adverse cardiovascular events; TAVR, transcatheter aortic valve replacement.

Robustness verification

Bootstrap internal validation

Internal validation using 1,000 bootstrap resamples showed that the apparent C-index of the combined model was 0.751, and the bias-corrected value was 0.742, with an optimism bias of only 0.008. The apparent 24-month AUC was 0.757, and the optimism-corrected value was 0.762 (optimism −0.005). The results indicated low overfitting degree and good internal robustness. See Supplemental Table S9 for details.

Sensitivity analysis of perioperative events

After excluding 30-day perioperative events and refitting the model, high EAT remained an independent predictor of MACE ($P < 0.001$), with an increased effect size, further supporting that the predictive value of EAT for long-term events is more stable. The effect of high NPS weakened and was not statistically significant ($P = 0.229$). This result further verified the time-effect difference between the two: the prognostic effect of NPS is mainly in the early postoperative period, while EAT has more stable predictive value for long-term events. The combined model showed a 0.005 decrease in C-index and a 0.003 increase in the 24-month AUC compared with the primary analysis, indicating that the research conclusions are not interfered by perioperative events and have good robustness. See Supplemental Tables S10 and S11 for details.

Sensitivity analysis of exposure variable form

When EAT was modeled as a continuous variable instead of a binary variable, each 10 cm^3 increment was associated with a 16% higher risk of MACE (HR 1.16, 95% CI 1.07–1.25, $P < 0.001$), and 17% in the combined model (HR 1.17, 95% CI 1.08–1.27, $P < 0.001$). The direction and statistical significance were consistent with the binary analysis, indicating that the prognostic effect of EAT is continuous and independent of the median cutoff (Supplemental Table S1).

Discussion

Main findings

In this single-center cohort of 427 patients with severe calcific aortic stenosis undergoing TAVR, both preoperative EAT volume and the NPS were independently associated with MACE, and their combination improved discrimination and reclassification beyond a conventional clinical risk model. The incremental value was driven mainly by improved discrimination (IDI) rather than by risk reclassification (NRI), which did not reach statistical

significance. EAT volume showed an approximately linear dose–response relationship with MACE, and the combined model provided stable risk stratification across the major clinical subgroups examined, with consistent results in multiple sensitivity analyses. To our knowledge, this study is among the first to evaluate the incremental predictive value of combining EAT volume and NPS over conventional clinical risk models in patients with severe aortic stenosis undergoing TAVR, providing evidence for simple preoperative risk stratification and individualized postoperative management. Time-varying coefficient analysis further showed that the effect of high EAT increased progressively over follow-up, whereas the effect of high NPS was confined to the early postoperative period, indicating that the two markers capture risk operating over different time windows.

An unexpected finding warrants comment: patients who developed MACE had a marginally higher DVI (0.22 vs 0.20) together with lower gradients. Both values were well within the severe range and the absolute difference was small, so the statistical significance mainly reflects sample size. A higher DVI with lower gradients is nonetheless compatible with reduced transvalvular flow, which may itself carry a worse prognosis. Because stroke volume was not recorded and DVI served only as an adjustment variable, this interpretation remains speculative.

Pathophysiological mechanism discussion

Local mechanism of EAT-mediated postoperative adverse events

Several mechanisms may explain why a higher preoperative EAT volume predisposes to adverse events after TAVR. A pro-inflammatory shift in EAT leads to the release of cytokines such as IL-1β, IL-6, TNF-α and MCP-1 that promote myocardial fibrosis, valve calcification and electrical conduction abnormalities [16–18]. Mazurek et al. [16] showed that expression of these inflammatory factors in EAT was significantly higher than in subcutaneous fat and independent of circulating inflammatory markers, indicating that EAT is an independent local

inflammatory source of the heart. In calcific aortic stenosis, mediators secreted by EAT diffuse to the valve leaflets and promote osteogenic differentiation and calcification of valve interstitial cells; Parisi et al. [22] and Nabati et al. [23] both reported that greater EAT thickness was associated with more severe valve sclerosis and left ventricular dysfunction. After TAVR, persistent EAT-mediated inflammation may impair endothelialization of the prosthesis, aggravate myocardial interstitial fibrosis and delay reverse left ventricular remodeling, thereby increasing the risk of heart failure rehospitalization and late cardiovascular events. Consistent with this, we observed a continuous dose–response relationship between EAT volume and MACE (non-linearity $P = 0.092$; HR 1.16 per 10 cm^3), in line with a meta-analysis of 29 studies [19], with reports linking higher EAT volume to impaired left atrial reservoir function in severe aortic stenosis [50], and with evidence that EAT is associated with myocardial remodeling and adverse prognosis in asymptomatic aortic stenosis [54]. Notably, the two markers showed distinct time-dependent behavior: the effect of high EAT increased progressively over follow-up (HR 3.64 at 3 months to 7.84 at 60 months), which also explains why the proportional hazards assumption was violated once EAT entered the model, whereas the effect of high NPS was confined to the early postoperative period. This suggests different clinical windows: perioperative optimization, nutritional support and infection control for patients with a high NPS, and long-term anti-inflammatory and reverse-remodeling strategies for those with high EAT.

Systemic effect of NPS reflecting immune and nutritional reserve

NPS integrates four routine laboratory indices — serum albumin, total cholesterol, NLR and LMR — and therefore reflects both nutritional reserve and chronic inflammatory activation, with higher scores indicating greater inflammation and poorer nutritional reserve [34]. Serum albumin is a core marker of nutritional status and low total cholesterol is typical of chronic inflammatory consumption, while the composite score that incorporates NLR and LMR has

been consistently associated with adverse cardiovascular outcomes [39, 40]. In patients undergoing TAVR, preoperative malnutrition and chronic low-grade inflammation together impair tissue healing, dysregulate the inflammatory response and promote myocardial remodeling and worsening cardiac function, ultimately contributing to MACE [45]. Compared with single inflammatory or nutritional markers, the NPS covers more dimensions while requiring only routine preoperative laboratory tests, making it highly accessible. In TAVR cohorts, a high NPS has been associated with increased 1-year mortality [43] and with 1-year MACE [42], and its core component NLR has likewise been linked to short- and long-term mortality after TAVR in large cohorts and meta-analyses [44]. In the present study, a high NPS was an independent predictor of MACE (HR 1.96, 95% CI 1.27–3.04; $P = 0.003$), consistent with these findings. Perioperative sensitivity analysis supported the time-dependent nature of this effect: after excluding events within 30 days, the effect of high NPS attenuated to HR 1.43 and was no longer significant ($P = 0.229$), suggesting that the nutritional-inflammatory status captured by NPS mainly drives early postoperative complications and weakens as the patient recovers. This identifies a potential intervention window, in which perioperative nutritional support and control of infection and systemic inflammation may be the most effective way to reduce early adverse events in patients with a high NPS.

Dimensional complementarity of the combination

EAT volume and NPS were only weakly correlated (Spearman $r_s = 0.175$ for EAT volume vs. the high NPS category, $P < 0.001$), indicating limited information overlap. The two markers capture risk from different perspectives: EAT reflects the local cardiac fat load and paracrine inflammatory activity, whereas NPS reflects systemic immune-inflammatory activation and nutritional reserve [14, 45]. Although no statistical interaction was detected, the two markers may be linked biologically through a “local–systemic” inflammatory loop: cytokines released by EAT (for example IL-6, TNF-α and MCP-1) increase the systemic inflammatory burden

and consume nutritional reserve [16, 46], while systemic malnutrition and inflammation in turn promote a pro-inflammatory adipocyte phenotype in EAT and reduce protective adipokines such as adiponectin [17, 45]. This interplay may jointly drive myocardial interstitial fibrosis, endothelial dysfunction and ventricular remodeling, consistent with the view that EAT mediates the cardiac effects of systemic inflammation while systemic nutritional-inflammatory status modulates EAT [45, 46]. This dimensional complementarity provides the pathophysiological basis for the improvement in model performance when the two markers are combined.

Comparison with previous studies

Prognostic value of EAT in TAVR is consistent with previous studies

Previous TAVR cohorts have consistently shown that a higher EAT volume, EAT density or EAT thickness is associated with adverse outcomes [27–30], and the present findings are in line with these observations. However, most previous studies adopted all-cause mortality as the primary endpoint, while this study further validates the predictive value of EAT for the composite endpoint of MACE. In terms of the dose–response relationship, the restricted cubic spline model of this study demonstrates an overall linear trend with marginal non-linear characteristics. This not only supports a continuous dose-dependent association between EAT and risk, but also suggests a potential accelerated rise in risk at higher volume ranges, which requires verification with larger sample sizes. In addition, the mean EAT volume of the population in this study was 108.15 cm^3, lower than the high-risk cutoff value of 130 cm^3 reported in previous studies, indicating that the prognostic value of EAT is already evident even at moderate volume levels. Automated artificial intelligence-based and combined adipose-muscle assessments may further refine risk prediction after TAVR [55, 56]. Consistent findings have also been reported in asymptomatic aortic stenosis, in which EAT was associated with cardiac remodeling and clinical outcomes [57].

Prognostic value of NPS in TAVR population is verified

Since its original description in patients undergoing colorectal cancer surgery [34], the NPS has been validated in several TAVR cohorts, in which a high score was associated with increased 1-year mortality and MACE [41–43]; the present results are consistent with these observations. Furthermore, after adjusting for EAT volume, NPS remained an independent predictor of MACE, indicating that its prognostic value does not depend on the level of local fat inflammation, and their effects are independent of each other.

Incremental value of the combined model

Most existing studies have separately verified the prognostic value of EAT or NPS as a single marker, and the incremental predictive value of their combination on traditional risk scores has not been reported. This study showed that after adding both EAT and NPS to EuroSCORE II, the C-index increased from 0.716 to 0.751. Likelihood ratio test confirmed significant improvement in model fit. Both NRI and IDI were positive, although only the IDI reached statistical significance, indicating that the incremental value of the two markers was driven mainly by improved overall discrimination rather than by risk reclassification. Previous large-scale validation studies have shown that traditional surgical risk scores such as EuroSCORE II and STS-PROM mainly focus on perioperative mortality risk, with limited predictive performance for long-term cardiovascular events after TAVR. Their C-index is mostly between 0.60 and 0.67, and there is generally calibration bias [11, 13]. In this study, the C-index of the baseline clinical model was 0.716, which is at a relatively high level among similar studies. The improvement after adding the two simple markers is significant, and both indicators can be directly obtained from routine preoperative examinations without additional tests, with high clinical transformation value.

Clinical implications

This study has several potential clinical implications. First, it provides a simple preoperative risk-stratification tool: EAT volume can be quantified from routine preoperative aortic CTA

without additional scanning, and NPS can be derived from routine blood counts and biochemistry, so both are low-cost, readily accessible and easy to interpret. Combined assessment can therefore identify patients at high risk of MACE after TAVR and complement traditional surgical risk scores, which do not capture inflammation or nutritional status. Second, it may guide stratified postoperative management: patients with low EAT and low NPS may be suitable for routine follow-up, whereas those with both markers elevated could benefit from closer surveillance of cardiac function and volume status together with targeted nutritional support and anti-inflammatory management, particularly because heart failure rehospitalization was the most common MACE component in this cohort. Finally, it provides a new direction for TAVR prognostic modeling; future multicenter studies with larger samples could integrate EAT volume and NPS into a visual nomogram for bedside risk calculation.

Study limitations

This study has several limitations. First, it was a single-center retrospective cohort study, which may introduce selection bias. The limited sample size and number of MACE events may reduce statistical power, particularly for conservative incremental measures such as NRI. The bicuspid aortic valve subgroup was especially small (n = 50; 8 MACE events), limiting statistical power and requiring validation in multicenter cohorts. Second, EAT volume was quantified using a single-center scanning protocol with good intra-center reproducibility but limited cross-center generalizability; a standardized multicenter measurement protocol is needed [58]. Third, for local imaging assessment, only EAT volume was included; EAT density and radiomic features were not evaluated, and individual components of the composite MACE endpoint were not analyzed separately [51, 59]. Fourth, Models 2 and 4 violated the proportional hazards assumption and the EAT variable showed evidence of time-varying effects, so the standard Cox hazard ratios should be interpreted as average effects

over follow-up. We explored this with a time-varying coefficient model, which showed that the effect of high EAT increased over follow-up whereas that of high NPS was confined to the early postoperative period (Supplemental Table S6 and Fig. 7). These time-specific estimates are exploratory and require confirmation in larger cohorts, in which restricted mean survival time or landmark analyses could also be applied. Finally, as an observational study, this work can establish associations but cannot confirm causality or clarify the mechanisms linking preoperative EAT volume and NPS to MACE after TAVR.

Conclusions

In summary, this study confirms that preoperative EAT volume and the NPS are both independent predictors of major adverse cardiovascular events after TAVR in patients with severe calcific aortic valve stenosis. The two factors provide complementary prognostic information from the perspectives of local inflammation and systemic immune-inflammation, and their combined application can significantly improve the predictive performance of traditional clinical risk models. The combined model showed good discrimination, acceptable calibration and clear clinical net benefit, and it maintained stable risk stratification in the major clinical subgroups examined. Multiple sensitivity analyses supported the robustness of these conclusions. The linear dose–response characteristic of EAT and the temporal heterogeneity of their prognostic effects identified by the study can provide a theoretical basis for clinical stratified intervention. This assessment scheme is simple and accessible, and can serve as an auxiliary tool for preoperative risk stratification and postoperative individualized management of TAVR. Its conclusions need further verification by multicenter large-sample cohorts, and the long-term value of targeted intervention deserves in-depth exploration.

Abbreviations

AUC, area under the receiver operating characteristic curve; BMI, body mass index; CAVD, calcific aortic valve disease; CI, confidence interval; C-index, concordance index; COPD,

chronic obstructive pulmonary disease; Cr, creatinine; CT, computed tomography; CTA, computed tomography angiography; DCA, decision curve analysis; DVI, Doppler velocity index; EAT, epicardial adipose tissue; eGFR, estimated glomerular filtration rate; EuroSCORE II, European System for Cardiac Operative Risk Evaluation II; HDL-C, high-density lipoprotein cholesterol; HR, hazard ratio; ICC, intraclass correlation coefficient; IDI, integrated discrimination improvement; IL-1β, interleukin-1β; IL-6, interleukin-6; IQR, interquartile range; LDL-C, low-density lipoprotein cholesterol; LMR, lymphocyte-to-monocyte ratio; LVEF, left ventricular ejection fraction; MACE, major adverse cardiovascular events; MCP-1, monocyte chemoattractant protein-1; NLR, neutrophil-to-lymphocyte ratio; NPS, Naples Prognostic Score; NRI, net reclassification index; NT-proBNP, N-terminal pro-B-type natriuretic peptide; NYHA, New York Heart Association; PCI, percutaneous coronary intervention; PH, proportional hazards; RCS, restricted cubic spline; ROC, receiver operating characteristic; SD, standard deviation; STROBE, Strengthening the Reporting of Observational Studies in Epidemiology; STS-PROM, Society of Thoracic Surgeons Predicted Risk of Mortality; TAVR, transcatheter aortic valve replacement; TNF-α, tumor necrosis factor-α; VARC-3, Valve Academic Research Consortium 3; VIF, variance inflation factor; WBC, white blood cell count.

Declarations

Ethics approval and consent to participate

The studies involving human participants were reviewed and approved by the Medical Ethics Committee of the Affiliated Hospital of Qingdao University (approval No. QYFYWZLL50843). This retrospective study used anonymized data derived from routine clinical practice; written informed consent for participation was therefore not required, in accordance with the national legislation and the institutional requirements.

Consent for publication

Not applicable.

Availability of data and materials

The de-identified dataset and the R code supporting the conclusions of this article are available from the corresponding author on reasonable request, subject to approval by the institutional ethics committee and a signed data-use agreement. Raw CT images cannot be shared because they contain potentially identifying information.

Competing interests

The authors declare that the research was conducted in the absence of any commercial or financial relationships that could be construed as a potential conflict of interest.

Funding

No specific funding was received for this work.

Authors' contributions

BC, LX, LK, ZC, XZ and LZ all made substantial contributions to the study. BC was responsible for conceptualization, methodology, investigation, formal analysis and writing of the original draft. LX contributed to investigation and formal analysis. LK contributed to investigation and data curation. ZC contributed to formal analysis and visualization. XZ contributed to visualization and to writing (review and editing). LZ supervised the study and contributed to writing (review and editing). All authors read and approved the final version of the manuscript.

Acknowledgements

The authors thank all patients who participated in this study and the staff of the Department of Cardiology and the Department of Radiology of the Affiliated Hospital of Qingdao University for their assistance with data collection and image analysis.

Additional files

Additional file 1: Supplemental material, including Supplemental Methods, Supplemental Tables S1–S11 and Supplemental Figures S1–S3 (PDF).

Additional file 2: STROBE Statement checklist for cohort studies, indicating the page number of each reported item (DOCX).

References

842

843 1. Cho KI, Sakuma I, Sohn IS, Jo S-H, Koh KK. Inflammatory and metabolic mechanisms
844 underlying the calcific aortic valve disease. Atherosclerosis. 2018;277:60–5.
845 https://doi.org/10.1016/j.atherosclerosis.2018.08.029.

846 2. Moncla L-HM, Briend M, Bossé Y, Mathieu P. Calcific aortic valve disease: mechanisms,
847 prevention and treatment. Nat Rev Cardiol. 2023;20:546–59. https://doi.org/10.1038/s41569-
848 023-00845-7.

849 3. Conte M, Petraglia L, Campana P, Gerundo G, Caruso A, Grimaldi MG, et al. The role of
850 inflammation and metabolic risk factors in the pathogenesis of calcific aortic valve stenosis.
851 Aging Clin Exp Res. 2021;33:1765–70. https://doi.org/10.1007/s40520-020-01681-2.

852 4. Yadgir S, Johnson CO, Aboyans V, Adebayo OM, Adedoyin RA, Afarideh M, et al.
853 Global, regional, and national burden of calcific aortic valve and degenerative mitral valve
854 diseases, 1990-2017. Circulation. 2020;141:1670–80.
855 https://doi.org/10.1161/CIRCULATIONAHA.119.043391.

856 5. Lindman BR, Clavel M-A, Mathieu P, Iung B, Lancellotti P, Otto CM, et al. Calcific aortic
857 stenosis. Nat Rev Dis Primers. 2016;2:16006. https://doi.org/10.1038/nrdp.2016.6.

858 6. Otto CM, Newby DE, Hillis GS. Calcific aortic stenosis: a review. JAMA. 2024;332:2014–
859 26. https://doi.org/10.1001/jama.2024.16477.

860 7. Vahanian A, Beyersdorf F, Praz F, Milojevic M, Baldus S, Bauersachs J, et al. 2021
861 ESC/EACTS Guidelines for the management of valvular heart disease: Developed by the
862 Task Force for the management of valvular heart disease of the European Society of
863 Cardiology (ESC) and the European Association for Cardio-Thoracic Surgery (EACTS). Eur
864 Heart J. 2022;43:561–632. https://doi.org/10.1093/eurheartj/ehab395.

8. Praz F, Borger MA, Lanz J, Marin-Cuartas M, Abreu A, Adamo M, et al. 2025 ESC/EACTS Guidelines for the management of valvular heart disease. Eur Heart J. 2025;46:4635–736. https://doi.org/10.1093/eurheartj/ehaf194.

9. Thyregod HGH, Jørgensen TH, Ihlemann N, Steinbrüchel DA, Nissen H, Kjeldsen BJ, et al. Transcatheter or surgical aortic valve implantation: 10-year outcomes of the NOTION trial. Eur Heart J. 2024;45:1116–24. https://doi.org/10.1093/eurheartj/ehae043.

10. Généreux P, Schwartz A, Oldemeyer JB, Pibarot P, Cohen DJ, Blanke P, et al. Transcatheter aortic-valve replacement for asymptomatic severe aortic stenosis. N Engl J Med. 2025;392:217–27. https://doi.org/10.1056/NEJMoa2405880.

11. Wolff G, Shamekhi J, Al-Kassou B, Tabata N, Parco C, Klein K, et al. Risk modeling in transcatheter aortic valve replacement remains unsolved: an external validation study in 2946 German patients. Clin Res Cardiol. 2021;110:368–76. https://doi.org/10.1007/s00392-020-01731-9.

12. Duncan A, Ludman P, Banya W, Cunningham D, Marlee D, Davies S, et al. Long-term outcomes after transcatheter aortic valve replacement in high-risk patients with severe aortic stenosis: the U.K. Transcatheter Aortic Valve Implantation Registry. JACC Cardiovasc Interv. 2015;8:645–53. https://doi.org/10.1016/j.jcin.2015.01.009.

13. Kreutz J, Lauten P, Chatzis G, Nabrotzki M, Patsalis N, Syntila S, et al. Patient risk evaluation for transcatheter aortic valve replacement (PRE-TAVR) — identification of real-time predictors of short- and long-term mortality. Clin Res Cardiol. 2025;114:1574–84. https://doi.org/10.1007/s00392-025-02704-6.

14. Oikonomou EK, Antoniades C. The role of adipose tissue in cardiovascular health and disease. Nat Rev Cardiol. 2019;16:83–99. https://doi.org/10.1038/s41569-018-0097-6.

15. Iacobellis G. Epicardial adipose tissue in contemporary cardiology. Nat Rev Cardiol. 2022;19:593–606. https://doi.org/10.1038/s41569-022-00679-9.

16. Mazurek T, Zhang L, Zalewski A, Mannion JD, Diehl JT, Arafat H, et al. Human epicardial adipose tissue is a source of inflammatory mediators. Circulation. 2003;108:2460–6. https://doi.org/10.1161/01.CIR.0000099542.57313.C5.

17. Packer M. Epicardial adipose tissue may mediate deleterious effects of obesity and inflammation on the myocardium. J Am Coll Cardiol. 2018;71:2360–72. https://doi.org/10.1016/j.jacc.2018.03.509.

18. Ernault AC, Meijborg VMF, Coronel R. Modulation of cardiac arrhythmogenesis by epicardial adipose tissue: JACC state-of-the-art review. J Am Coll Cardiol. 2021;78:1730–45. https://doi.org/10.1016/j.jacc.2021.08.037.

19. Chong B, Jayabaskaran J, Ruban J, Goh R, Chin YH, Kong G, et al. Epicardial adipose tissue assessed by computed tomography and echocardiography are associated with adverse cardiovascular outcomes: a systematic review and meta-analysis. Circulation: Cardiovascular Imaging. 2023;16:e015159. https://doi.org/10.1161/CIRCIMAGING.122.015159.

20. van Woerden G, van Veldhuisen DJ, Westenbrink BD, de Boer RA, Rienstra M, Gorter TM. Connecting epicardial adipose tissue and heart failure with preserved ejection fraction: mechanisms, management and modern perspectives. Eur J Heart Fail. 2022;24:2238–50. https://doi.org/10.1002/ejhf.2741.

21. Khanna S, Mann G, Bhat A, Lin A, Patel A, Nicholls SJ, et al. Role of systemic and epicardial adipose tissue in cardiometabolic disease. Nat Rev Cardiol. 2026;23:413–431. https://doi.org/10.1038/s41569-026-01304-9.

22. Parisi V, Rengo G, Pagano G, D'Esposito V, Passaretti F, Caruso A, et al. Epicardial adipose tissue has an increased thickness and is a source of inflammatory mediators in

912 patients with calcific aortic stenosis. Int J Cardiol. 2015;186:167–169.
913 https://doi.org/10.1016/j.ijcard.2015.03.201.

914 23. Nabati M, Favaedi M, Kheirgoo M, Yazdani J, Dabirian M. Correlation between
915 epicardial fat thickness and aortic valve sclerosis. Asian Cardiovasc Thorac Ann.
916 2018;26:188–95. https://doi.org/10.1177/0218492318760692.

917 24. Mahabadi AA, Kahlert HA, Dykun I, Balcer B, Kahlert P, Rassaf T. Epicardial adipose
918 tissue thickness independently predicts severe aortic valve stenosis. J Heart Valve Dis.
919 2017;26:262–7.

920 25. Davin L, Nchimi A, Ilardi F, Dulgheru R, Marchetta S, Gach O, et al. Epicardial adipose
921 tissue and myocardial fibrosis in aortic stenosis relationship with symptoms and outcomes: a
922 study using cardiac magnetic resonance imaging. JACC Cardiovasc Imaging. 2019;12:213–4.
923 https://doi.org/10.1016/j.jcmg.2018.06.025.

924 26. Hardt F, Becker M, Brandenburg V, Grebe J, Dirrichs T, Gohmann RF, et al. Impact of
925 epicardial adipose tissue volume upon left ventricular dysfunction in patients with mild-to-
926 moderate aortic stenosis: A post-hoc analysis. PLoS One. 2020;15:e0229636.
927 https://doi.org/10.1371/journal.pone.0229636.

928 27. Eberhard M, Stocker D, Meyer M, Kebernik J, Stähli BE, Frauenfelder T, et al. Epicardial
929 adipose tissue volume is associated with adverse outcomes after transcatheter aortic valve
930 replacement. Int J Cardiol. 2019;286:29–35. https://doi.org/10.1016/j.ijcard.2019.01.068.

931 28. Schulz A, Beuthner BE, Böttiger ZM, Gersch SS, Lange T, Gronwald J, et al. Epicardial
932 adipose tissue as an independent predictor of long-term outcome in patients with severe aortic
933 stenosis undergoing transcatheter aortic valve replacement. Clin Res Cardiol. 2025;114:1467–
934 78. https://doi.org/10.1007/s00392-024-02387-5.

935 29. Salam B, Al-Kassou B, Weinhold L, Sprinkart AM, Nowak S, Theis M, et al. CT-derived
936 epicardial adipose tissue inflammation predicts outcome in patients undergoing transcatheter
937 aortic valve replacement. J Thorac Imaging. 2024;39:224–31.
938 https://doi.org/10.1097/RTI.0000000000000776.

939 30. Piña P, Lorenzatti D, Filtz A, Scotti A, Gil EV, Torres JD, et al. Epicardial adipose tissue,
940 cardiac damage, and mortality in patients undergoing TAVR for aortic stenosis. Int J
941 Cardiovasc Imaging. 2025;41:279–90. https://doi.org/10.1007/s10554-024-03307-4.

942 31. Ertaş G, Ekmekçi A, Şahin S, Murat A, Bakhshaliyev N, Erer HB, et al. Epicardial fat
943 thickness assessment by multi-slice computed tomography for predicting cardiac outcomes in
944 patients undergoing transcatheter aortic valve implantation. Cardiovasc J Afr. 2022;33:108–
945 11. https://doi.org/10.5830/CVJA-2021-043.

946 32. Rohrbach S, Uluocak O, Junge M, Knapp F, Schulz R, Böning A, et al. Epicardial adipose
947 tissue and muscle distribution affect outcomes in very old patients after transcatheter aortic
948 valve replacement. Eur Heart J Open. 2024;4:oeae073.
949 https://doi.org/10.1093/ehjopen/oeae073.

950 33. Storozhenko T, Buytaert D, Mistrulli R, Viscusi MM, Corradetti S, Fiori E, et al. Imaging
951 and biomarker-based risk stratification in TAVI: the role of epicardial fat, visceral fat, and
952 adiponectin. Eur Heart J Open. 2026;6:oeag085. https://doi.org/10.1093/ehjopen/oeag085.

953 34. Galizia G, Lieto E, Auricchio A, Cardella F, Mabilia A, Podzemny V, et al. Naples
954 prognostic score, based on nutritional and inflammatory status, is an independent predictor of
955 long-term outcome in patients undergoing surgery for colorectal cancer. Dis Colon Rectum.
956 2017;60:1273–84. https://doi.org/10.1097/DCR.0000000000000961.

957 35. Galizia G, Auricchio A, de Vita F, Cardella F, Mabilia A, Basile N, et al. Inflammatory
958 and nutritional status is a predictor of long-term outcome in patients undergoing surgery for
959 gastric cancer. Validation of the Naples prognostic score. Ann Ital Chir. 2019;90:404–16.

960 36. Feng J-F, Zhao J-M, Chen S, Chen Q-X. Naples prognostic score: a novel prognostic
961 score in predicting cancer-specific survival in patients with resected esophageal squamous cell
962 carcinoma. Front Oncol. 2021;11:652537. https://doi.org/10.3389/fonc.2021.652537.

963 37. Yang J, Lv L, Zhao F, Mei X, Zhou H, Yu F. The value of the preoperative Naples
964 prognostic score in predicting prognosis in gallbladder cancer surgery patients. World J Surg
965 Oncol. 2023;21:303. https://doi.org/10.1186/s12957-023-03198-0.

966 38. Wang Y, Hu X, Zheng D, Shao Y, Lia T, Li X. Prognostic significance of Naples
967 prognostic score in operable renal cell carcinoma. Front Surg. 2022;9:969798.
968 https://doi.org/10.3389/fsurg.2022.969798.

969 39. Kılıç O, Suygun H, Mustu M, Ozpamuk Karadeniz F, Ozer SF, Senol H, et al. Is the
970 Naples prognostic score useful for predicting heart failure mortality. Kardiologiia.
971 2023;63:61–5. https://doi.org/10.18087/cardio.2023.3.n2328.

972 40. Erdogan A, Genc O, Ozkan E, Goksu MM, Ibisoglu E, Bilen MN, et al. Impact of Naples
973 prognostic score at admission on in-hospital and follow-up outcomes among patients with ST-
974 segment elevation myocardial infarction. Angiology. 2023;74:970–80.
975 https://doi.org/10.1177/00033197231151559.

976 41. Çetin ZG, Balun A, Çiçekçioğlu H, Demirtaş B, Yiğitbaşı MM, Özbek K, et al. A novel
977 score to predict one-year mortality after transcatheter aortic valve replacement, Naples
978 prognostic score. Medicina (Kaunas). 2023;59:1666.
979 https://doi.org/10.3390/medicina59091666.

42. Gitmez M, Güzel T, Kis M, Coskun F, İsik MA, Aktan A, et al. The performance of the NAPLES prognostic score in predicting one-year mortality and major adverse cardiovascular events after transcatheter aortic valve implantation in patients with severe aortic stenosis. Kardiol Pol. 2025;83:287–94. https://doi.org/10.33963/v.phj.103230.

43. Demirci G, Aslan S, Güner A, Demir AR, Erata YE, Türkmen İ, et al. Clinical implication of the Naples prognostic score on transcatheter aortic valve replacement in patients with severe aortic stenosis. Catheter Cardiovasc Interv. 2024;103:219–25. https://doi.org/10.1002/ccd.30929.

44. Rawat A, Goyal P, Ahsan SA, Surya Srivyshnavi KS, Hannan Asghar A, Riyalat AA, et al. The prognostic value of neutrophil-to-lymphocyte ratio on mortality in patients undergoing transcatheter aortic valve implantation: a systematic review and meta-analysis. Cureus. 2025;17:e77909. https://doi.org/10.7759/cureus.77909.

45. Conte M, Petraglia L, Poggio P, Valerio V, Cabaro S, Campana P, et al. Inflammation and cardiovascular diseases in the elderly: the role of epicardial adipose tissue. Front Med (Lausanne). 2022;9:844266. https://doi.org/10.3389/fmed.2022.844266.

46. González N, Moreno-Villegas Z, González-Bris A, Egido J, Lorenzo Ó. Regulation of visceral and epicardial adipose tissue for preventing cardiovascular injuries associated to obesity and diabetes. Cardiovasc Diabetol. 2017;16:44. https://doi.org/10.1186/s12933-017-0528-4.

47. von Elm E, Altman DG, Egger M, Pocock SJ, Gøtzsche PC, Vandenbroucke JP, et al. The Strengthening the Reporting of Observational Studies in Epidemiology (STROBE) statement: guidelines for reporting observational studies. J Clin Epidemiol. 2008;61:344–9. https://doi.org/10.1016/j.jclinepi.2007.11.008.

48. Li X, Sun Y, Xu L, Greenwald SE, Zhang L, Zhang R, et al. Automatic quantification of epicardial adipose tissue volume. Medical Physics. 2021;48:4279–90. https://doi.org/10.1002/mp.15012.

49. Marwan M, Achenbach S. Quantification of epicardial fat by computed tomography: Why, when and how? J Cardiovasc Comput Tomogr. 2013;7:3–10. https://doi.org/10.1016/j.jcct.2013.01.002.

50. Gronwald J, Lange T, Backhaus SJ, Beuthner BE, Evertz R, Puls M, et al. Impact of epicardial adipose tissue on myocardial function and structure in patients with severe aortic valve stenosis. ESC Heart Fail. 2025;12:4230–41. https://doi.org/10.1002/ehf2.15422.

51. Sato T, Yufu K, Yamasaki H, Harada T, Yamauchi S, Ishii Y, et al. Quality of epicardial adipose tissue predicts major adverse cerebral and cardiovascular events following transcatheter aortic valve implantation. Heart Vessels. 2024;39:646–53. https://doi.org/10.1007/s00380-024-02374-w.

52. Nashef SAM, Roques F, Sharples LD, Nilsson J, Smith C, Goldstone AR, et al. EuroSCORE II. Eur J Cardiothorac Surg. 2012;41:734–44; discussion 744-745. https://doi.org/10.1093/ejcts/ezs043.

53. VARC-3 WRITING COMMITTEE, Généreux P, Piazza N, Alu MC, Nazif T, Hahn RT, et al. Valve Academic Research Consortium 3: updated endpoint definitions for aortic valve clinical research. Eur Heart J. 2021;42:1825–57. https://doi.org/10.1093/eurheartj/ehaa799.

54. Geers J, Manral N, Razipour A, Park C, Tomasino GF, Xing E, et al. Epicardial adipose tissue, myocardial remodelling and adverse outcomes in asymptomatic aortic stenosis. Heart. 2025;111:686–94. https://doi.org/10.1136/heartjnl-2024-324925.

55. Tremamunno G, Vecsey-Nagy M, Schoepf UJ, Zsarnoczay E, Aquino GJ, Kravchenko D, et al. Artificial intelligence improves prediction of major adverse cardiovascular events in

1027 patients undergoing transcatheter aortic valve replacement planning CT. Acad Radiol.
1028 2025;32:702–11. https://doi.org/10.1016/j.acra.2024.09.046.

1029 56. Walpot J, Van Herck P, Van de Heyning CM, Bosmans J, Massalha S, Malbrain MLNG,
1030 et al. Computed tomography measured epicardial adipose tissue and psoas muscle attenuation:
1031 new biomarkers to predict major adverse cardiac events (MACE) and mortality in patients
1032 with heart disease and critically ill patients. Part I: Epicardial adipose tissue. Anaesthesiol
1033 Intensive Ther. 2023;55:141–57. https://doi.org/10.5114/ait.2023.130922.

1034 57. Ayton SL, Aslam S, Dattani A, Yeo JL, Gulsin GS, Slomka PJ, et al. Association of
1035 epicardial adipose tissue with markers of cardiac remodelling and clinical outcomes in
1036 asymptomatic aortic stenosis. Open Heart. 2026;13:e003804. https://doi.org/10.1136/openhrt-
1037 2025-003804.

1038 58. West HW, Siddique M, Williams MC, Volpe L, Desai R, Lyasheva M, et al. Deep-
1039 learning for epicardial adipose tissue assessment with computed tomography. JACC
1040 Cardiovasc Imaging. 2023;16:800–16. https://doi.org/10.1016/j.jcmg.2022.11.018.

1041 59. Zhang Y, Yang HR, Ji XY, Xiong TY, Chen M. Radiomics of baseline epicardial adipose
1042 tissue predicts left ventricular mass regression after transcatheter aortic valve replacement. J
1043 Geriatr Cardiol. 2024;21:1109–18. https://doi.org/10.26599/1671-5411.2024.12.005.

Supplementary Files

This is a list of supplementary files associated with this preprint. Click to download.

- Additionalfile1.pdf